

Non-factorisable contributions of strong-penguin operators in $\Lambda_b \rightarrow \Lambda \ell^+ \ell^-$ decays

Thorsten Feldmann^a and Nico Gubernari^{a,b}

^a*Theoretische Physik 1, Center for Particle Physics Siegen, Universität Siegen,
Walter-Flex-Straße 3, 57068 Siegen, Germany*

^b*DAMTP, University of Cambridge,
Wilberforce Road, Cambridge, CB3 0WA, United Kingdom*

E-mail: thorsten.feldmann@uni-siegen.de, nicogubernari@gmail.com

ABSTRACT: We investigate for the first time a certain class of non-factorisable contributions of the four-quark operators \mathcal{O}_{3-6} in the weak effective Hamiltonian to the $\Lambda_b \rightarrow \Lambda \ell^+ \ell^-$ decay amplitude. We focus on the case where a virtual photon is radiated from one of the light constituents of the Λ_b baryon, in the kinematic situation of large hadronic recoil with an energetic Λ baryon in the final state. The effect on the suitably defined “non-local form factors” is calculated using the light-cone sum rule approach for a correlator with an interpolating current for the light Λ baryon. We find that this approach requires the introduction of new soft functions that generalise the standard light-cone distribution amplitudes (LCDAs) for the heavy Λ_b baryon. We give a heuristic discussion of their properties and a model that relates them to the standard LCDAs. Within this framework, we provide numerical results for the size of the non-local form factors considered.

KEYWORDS: Rare Decays, Specific QCD Phenomenology

ARXIV EPRINT: [2312.14146](https://arxiv.org/abs/2312.14146)

Contents

1	Introduction	1
2	Theoretical framework	4
2.1	Definition of local form factors	4
2.2	Definition of non-local form factors	5
2.3	Light-cone vectors and power counting	6
3	Calculation of the “annihilation topologies”	7
3.1	Definition of the correlator	7
3.2	Hadronic representation of the correlator	8
3.3	OPE analysis of the correlator	9
3.4	Λ_b soft functions with two light-like separations	12
3.5	Expressing the correlator in terms of soft functions	14
3.6	Derivation of light-cone sum rules	16
4	Numerical results	18
5	Conclusions	20
A	Models for Λ_b LCDAs in momentum space	21
B	Further details on the LCSRs	22

1 Introduction

Rare b -quark decays in general, and rare $b \rightarrow s\ell^+\ell^-$ transitions in particular, have received much attention in the past. From a phenomenological point of view, these decays provide a large number of complementary observables that allow us to explore the flavour sector of the Standard Model (SM) and its possible new-physics extensions (for comprehensive reviews, see e.g. refs. [1, 2] and references therein). From a theoretical point of view, the decays of a heavy quark into light degrees of freedom provide a valuable playground to develop and refine calculation methods to address the factorisation of hadronic bound-state effects from short-distance QCD corrections. In particular, one can establish QCD factorisation theorems (see e.g. refs. [3–5] for the pioneering works) for decay amplitudes of exclusive decays with large energy transfer to one or more light hadrons in the final state. Here, the bound-state effects are contained in hadronic transition form factors of local decay currents and light-cone distribution amplitudes (LCDAs) for light and heavy hadrons. Alternatively, it is possible to replace one or the other hadron by suitably chosen interpolating currents and relate the exclusive decay amplitude to the corresponding correlators by dispersion relations, namely the light-cone sum rule (LCSR) method (for a recent review, see ref. [6]). In both cases, the factorisation of “soft” degrees of freedom in the b -hadron and the energetic degrees of

freedom in the final state can be formally achieved by matching onto a soft-collinear effective theory (SCET), see e.g. refs. [7–9] for early applications in b -decays.

In the past, much of the phenomenological study of rare semileptonic $b \rightarrow s\ell^+\ell^-$ transitions has been devoted to exclusive $B \rightarrow K\ell^+\ell^-$ and $B \rightarrow K^*\ell^+\ell^-$ decays. In particular, a number of “flavour anomalies” (i.e. deviations between experimental measurements and theoretical expectations within the SM) may be due to physics beyond the SM, for recent reviews see refs. [10, 11]. However, a correct interpretation of these anomalies requires the control of systematic experimental effects as well as hadronic uncertainties in the theoretical predictions. For this reason, independent cross-checks of $b \rightarrow s\ell^+\ell^-$ transitions with complementary sensitivity to the different short-distance coefficients associated with the low-energy effective operators are desirable.

For instance, the angular analysis of baryonic transitions such as $\Lambda_b \rightarrow \Lambda(\rightarrow p\pi)\ell^+\ell^-$ [12] provides a number of independent observables [13, 14] that can be combined with data on mesonic decays in a global fit, see e.g. refs. [15, 16]. The most important hadronic input functions in these analyses are the $\Lambda_b \rightarrow \Lambda$ (local) transition form factors, which appear after factorising the (local) hadronic and leptonic currents in the semi-leptonic and electromagnetic penguin operators in the weak effective Hamiltonian, see the illustration in the left panel of figure 1. Quantitative results for the form factors can be obtained from lattice-QCD studies [17, 18] for small recoil energy (large invariant lepton mass squared q^2) and LCSRs for large recoil energy, see e.g. refs. [19–22]. Furthermore, one can exploit unitarity constraints in the form of a “ z -expansion”, which allows one to interpolate between small and large values of q^2 in a controlled way, see e.g. ref. [23]. Finally, in the heavy-quark limit for the b -quark, the number of independent form factors is reduced from ten to two at small recoil, and to only one at large recoil [21, 24, 25]. Note that the numerically dominant part of the form-factor values at large recoil is due to the so-called “soft-overlap” mechanism, where the energy transfer to the final state cannot be described by a finite number of virtual gluon exchanges (despite the fact that the latter mechanism is parametrically of leading power in QCD factorisation, see the discussion in ref. [26]).

Besides the local form-factor terms, time-ordered products of the hadronic operators in the weak effective Hamiltonian and the electromagnetic QED interaction also appear, leading to generalised hadronic matrix elements, often called “non-local form factors”. An important example in $b \rightarrow s\ell^+\ell^-$ transitions is the so-called “charm-loop effect”, where a $c\bar{c}$ pair is produced by a four-quark operator in the weak effective Hamiltonian and then annihilated by a virtual photon that subsequently decays into the charged lepton pair, see the illustration in the middle panel of figure 1. This effect restricts the perturbative treatment within QCD factorisation to values of q^2 well below the onset of charmonium resonances.¹ Nevertheless, phenomenological information about the lowest-lying $c\bar{c}$ resonances (J/ψ and ψ') can be implemented in a dispersive approach, which allows to extrapolate the perturbative results at small (or even negative) values to higher values of q^2 . This has been worked out in some detail for mesonic transitions, see e.g. refs. [28–30]. It is important to stress that

¹By a similar reasoning, the considered values of q^2 should be taken *above* the light vector resonances ρ, ω, \dots . An attempt to model the low- q^2 spectrum associated to annihilation topologies in rare D -meson decays within the QCD factorization approach has been discussed in ref. [27].

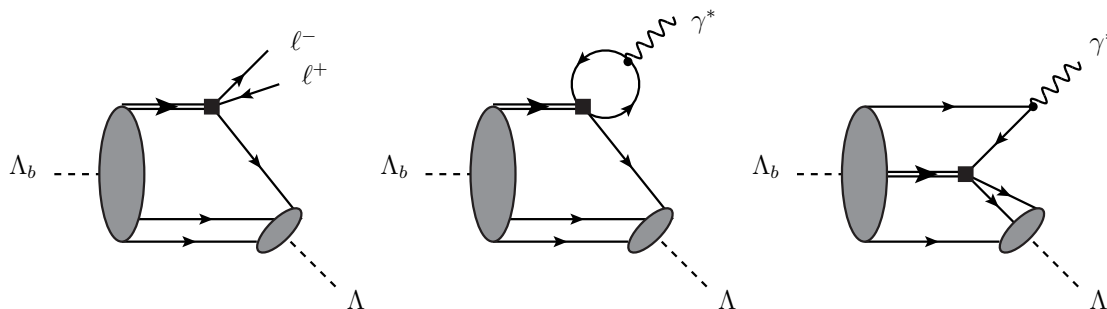


Figure 1. Illustration of different decay topologies for $\Lambda_b \rightarrow \Lambda \ell^+ \ell^-$: Left: local form-factor contribution for semi-leptonic operators \mathcal{O}_9 or \mathcal{O}_{10} . Center: Non-local contribution from virtual photon radiation off a charm (or light) quark loop. Right: example for a non-local contribution of the four-quark operators \mathcal{O}_{3-6} in $\Lambda_b \rightarrow \Lambda \ell^+ \ell^-$ decays. From the analogy to the corresponding terminology in $B \rightarrow K^{(*)} \ell^+ \ell^-$ decays, this is referred to as an “annihilation topology”. In each diagram, operators from the weak effective Hamiltonian are indicated by a black square, the b -quark is indicated by a double line, and the virtual photon subsequently dissociates into $\ell^+ \ell^-$ (not shown).

an adequate knowledge of the size of the non-local form factors in rare b -hadron decays is essential for a reliable estimate of theoretical uncertainties. Only the combination of accurate theoretical predictions and experimental measurements of rare flavour observables allows us to constrain the size of physics beyond the SM in these decays or even establish deviations from SM predictions.

In this work, we are interested in decay topologies like the one shown on the right panel of figure 1, for which there is no estimate to date. Here the four-quark operators \mathcal{O}_{3-6} connect two pairs of quarks in the initial and final baryon, with a virtual photon emitted from one of these quarks dissociating into $\ell^+ \ell^-$. This is analogous to the annihilation topologies in rare $B \rightarrow K^{(*)} \ell^+ \ell^-$ decays, and hence we refer to this contribution as “annihilation topologies”. From the example shown, it is immediately clear that the third valence quark (plus additional gluons or $q\bar{q}$ pairs) does not necessarily participate in the hard-scattering process. In the context of QCD factorisation [5] this would correspond to kinematic endpoint configurations which prevent a complete factorisation of the decay amplitude into hadronic LCDAs and short-distance kernels. In the following, we therefore consider the “annihilation topologies” in the framework of LCSRs with b -hadron LCDAs, following the procedures outlined in refs. [31, 32] for mesonic form factors and refs. [21, 22] for baryonic form factors.

The outline of this article is as follows. In section 2 we give our definitions of local and non-local form factors for the relevant operators in the weak effective Hamiltonian. We also introduce our kinematic notations and conventions that we use in the sum-rule calculation. In section 3 we introduce the correlator from which we deduce the contribution of the annihilation topologies by comparing the perturbative calculation in leading-order QCD with the hadronic representation in terms of non-local form factors. We find that the dominant effects are associated with the case where a virtual photon is emitted from one of the light-quarks in the Λ_b baryon. In this situation we find that the soft hadronic function describing the bound-state properties of the Λ_b baryon is given in terms of a tri-local operator where the two light-quark fields are separated along two *different* light-cone directions. We derive the

general momentum-space projector for this case in terms of generalised LCDAs. Section 4 is devoted to the numerical analysis of the sum rule with a careful assessment of parametric uncertainties from various sources. In comparison with the corresponding contribution of the local form-factor terms in the SM, we observe that the leading effect of the annihilation topologies is of similar size as in the mesonic counterpart for $B \rightarrow K\ell^+\ell^-$ or $B \rightarrow K_{\parallel}^*\ell^+\ell^-$. In fact, we find $\mathcal{O}(1\%)$ effects at the amplitude level for transverse γ^* polarisation, whereas the effect for longitudinal γ^* polarisation turns out to be negligible. After our conclusions in section 5, we provide some additional details about our modelling of the generalised LCDAs and some of the calculation steps in the sum-rule calculation in Appendices A and B.

2 Theoretical framework

2.1 Definition of local form factors

In $\Lambda_b \rightarrow \Lambda\ell^+\ell^-$ decays, the naively factorising contributions from the operators

$$\mathcal{O}_9 = \frac{\alpha_e}{4\pi} (\bar{s}\gamma^\mu P_L b) (\bar{\ell}\gamma_\mu \ell), \quad \mathcal{O}_{10} = \frac{\alpha_e}{4\pi} (\bar{s}\gamma^\mu P_L b) (\bar{\ell}\gamma_\mu \gamma_5 \ell), \quad (2.1)$$

in the weak effective Hamiltonian require the knowledge of the local transition form factors for vector and axial-vector $b \rightarrow s$ currents. Our conventions for these form factors in the helicity basis follow the definition in ref. [21]. For the vector form factor we use

$$\begin{aligned} \mathcal{F}_\mu \equiv \langle \Lambda(p') | \bar{s}\gamma_\mu b | \Lambda_b(p) \rangle = & \bar{u}_\Lambda(p') \left\{ f_0(q^2) (M_{\Lambda_b} - m_\Lambda) \frac{q_\mu}{q^2} \right. \\ & + f_+(q^2) \frac{M_{\Lambda_b} + m_\Lambda}{s_+} \left(p_\mu + p'_\mu - \frac{q_\mu}{q^2} (M_{\Lambda_b}^2 - m_\Lambda^2) \right) \\ & \left. + f_\perp(q^2) \left(\gamma_\mu - \frac{2m_\Lambda}{s_+} p_\mu - \frac{2m_{\Lambda_b}}{s_+} p'_\mu \right) \right\} u_{\Lambda_b}(p), \quad (2.2) \end{aligned}$$

where

$$s_\pm = (M_{\Lambda_b} \pm m_\Lambda)^2 - q^2. \quad (2.3)$$

An analogous definition holds for the form factors of axial-vector currents,

$$\begin{aligned} \mathcal{F}_{\mu 5} \equiv \langle \Lambda(p') | \bar{s}\gamma_\mu \gamma_5 b | \Lambda_b(p) \rangle = & -\bar{u}_\Lambda(p') \gamma_5 \left\{ g_0(q^2) (M_{\Lambda_b} + m_\Lambda) \frac{q_\mu}{q^2} \right. \\ & + g_+(q^2) \frac{M_{\Lambda_b} - m_\Lambda}{s_-} \left(p_\mu + p'_\mu - \frac{q_\mu}{q^2} (M_{\Lambda_b}^2 - m_\Lambda^2) \right) \\ & \left. + g_\perp(q^2) \left(\gamma_\mu + \frac{2m_\Lambda}{s_-} p_\mu - \frac{2m_{\Lambda_b}}{s_-} p'_\mu \right) \right\} u_{\Lambda_b}(p). \quad (2.4) \end{aligned}$$

Throughout this work the spin arguments for the fermion states and Dirac spinors are usually not explicitly shown for simplicity, i.e. $u_{\Lambda_b}(p, s) \equiv u_{\Lambda_b}(p)$. The projections on the vector form factors read

$$\begin{aligned} f_0(q^2) [\bar{u}_\Lambda(p') u_{\Lambda_b}(p)] &= \frac{q^\mu \mathcal{F}_\mu}{M_{\Lambda_b} - m_\Lambda}, \\ f_+(q^2) [\bar{u}_\Lambda(p') u_{\Lambda_b}(p)] &= -\frac{2q^2}{s_-} \frac{p^\mu \mathcal{F}_\mu}{M_{\Lambda_b} + m_\Lambda}, \\ f_\perp(q^2) [\bar{u}_\Lambda(p') \gamma'_\perp u_{\Lambda_b}(p)] &= g_\perp^{\nu\mu} \mathcal{F}_\mu, \quad (2.5) \end{aligned}$$

and similarly for the axial-vector form factors, where

$$g_{\perp}^{\mu\nu} = g^{\mu\nu} + \frac{4m_{\Lambda}^2}{s_+s_-} p^{\mu}p^{\nu} + \frac{4M_{\Lambda_b}^2}{s_+s_-} p'^{\mu}p'^{\nu} - \left(\frac{1}{s_+} + \frac{1}{s_-} \right) (p^{\mu}p'^{\nu} + p'^{\mu}p^{\nu})$$

is the metric tensor in the plane transverse to the momentum vectors p and p' .

2.2 Definition of non-local form factors

In this work, we are interested in hadronic matrix elements of the time-ordered product of the strong-penguin operators in the weak effective Hamiltonian

$$\begin{aligned} \mathcal{O}_3 &= (\bar{s}\gamma^{\nu}P_L b) \sum_q (\bar{q}\gamma_{\nu}P_L q), & \mathcal{O}_4 &= (\bar{s}^j\gamma^{\nu}P_L b^i) \sum_q (\bar{q}^i\gamma_{\nu}P_L q^j), \\ \mathcal{O}_5 &= (\bar{s}\gamma^{\nu}P_L b) \sum_q (\bar{q}\gamma_{\nu}P_R q), & \mathcal{O}_6 &= (\bar{s}^j\gamma^{\nu}P_L b^i) \sum_q (\bar{q}^i\gamma_{\nu}P_R q^j), \end{aligned} \quad (2.6)$$

with the electromagnetic current

$$J_{\mu}^{\text{em}}(x) = \sum_q Q_q \bar{q}(x) \gamma_{\mu} q(x), \quad (2.7)$$

where Q_q is the q quark charge. These matrix elements can be decomposed in the same way as the local form factors:

$$\begin{aligned} \mathcal{H}_{\mu}^{(i)} &= i \int d^4x e^{iq \cdot x} \langle \Lambda(p') | \mathcal{T} \{ \mathcal{O}_i(0) J_{\mu}^{\text{em}}(x) \} | \Lambda_b(p) \rangle \\ &\equiv M_{\Lambda_b}^2 \bar{u}_{\Lambda}(p') \left\{ \mathcal{H}_{+}^{(i)}(q^2) \frac{M_{\Lambda_b} + m_{\Lambda}}{s_+} \left(p_{\mu} + p'_{\mu} - \frac{q_{\mu}}{q^2} (M_{\Lambda_b}^2 - m_{\Lambda}^2) \right) \right. \\ &\quad \left. + \mathcal{H}_{\perp}^{(i)}(q^2) \left(\gamma_{\mu} - \frac{2m_{\Lambda}}{s_+} p_{\mu} - \frac{2M_{\Lambda_b}}{s_+} p'_{\mu} \right) \right\} u_{\Lambda_b}(p) \\ &\quad + M_{\Lambda_b}^2 \bar{u}_{\Lambda}(p') \gamma_5 \left\{ \mathcal{H}_{+5}^{(i)}(q^2) \frac{M_{\Lambda_b} - m_{\Lambda}}{s_-} \left(p_{\mu} + p'_{\mu} - \frac{q_{\mu}}{q^2} (M_{\Lambda_b}^2 - m_{\Lambda}^2) \right) \right. \\ &\quad \left. + \mathcal{H}_{\perp 5}^{(i)}(q^2) \left(\gamma_{\mu} + \frac{2m_{\Lambda}}{s_-} p_{\mu} - \frac{2M_{\Lambda_b}}{s_-} p'_{\mu} \right) \right\} u_{\Lambda_b}(p). \end{aligned} \quad (2.8)$$

Notice that due to the conservation of the electromagnetic current, Lorentz structures proportional to q^{μ} do not appear on the r.h.s. of this equation. In the following, we use the term “non-local form factors” for the generalised objects $\mathcal{H}_{+5}^{(i)}$ and $\mathcal{H}_{\perp 5}^{(i)}$. These non-local form factors can be isolated by contracting eq. (2.8) with p^{μ} and $g_{\perp}^{\mu\nu}$, respectively. These projections read

$$\begin{aligned} p^{\mu} \mathcal{H}_{\mu}^{(i)} &= -\frac{M_{\Lambda_b}^2}{2q^2} u_{\Lambda}(p') \left[s_-(M_{\Lambda_b} + m_{\Lambda}) \mathcal{H}_{+}^{(i)}(q^2) - s_+(M_{\Lambda_b} - m_{\Lambda}) \mathcal{H}_{+5}^{(i)}(q^2) \gamma_5 \right] u_{\Lambda_b}(p), \\ g_{\perp}^{\mu\nu} \mathcal{H}_{\mu}^{(i)} &= M_{\Lambda_b}^2 u_{\Lambda}(p') \left[\mathcal{H}_{\perp}^{(i)}(q^2) \gamma_{\perp}^{\nu} - \mathcal{H}_{\perp 5}^{(i)}(q^2) \gamma_{\perp}^{\nu} \gamma_5 \right] u_{\Lambda_b}(p). \end{aligned} \quad (2.9)$$

With these conventions, the non-local contributions to the $\Lambda_b \rightarrow \Lambda \ell^+ \ell^-$ decay amplitude can be rewritten in terms of a q^2 dependent shift of C_9 . Hence they can be accounted for

using the following replacements:

$$C_9 f_+(q^2) \rightarrow C_9 f_+(q^2) - 16\pi^2 \frac{2M_{\Lambda_b}^2}{q^2} \sum_i C_i \mathcal{H}_+^{(i)}(q^2) \equiv f_+(q^2) \left(C_9 + \Delta C_{9,+}(q^2) \right), \quad (2.10)$$

$$C_9 f_\perp(q^2) \rightarrow C_9 f_\perp(q^2) - 16\pi^2 \frac{2M_{\Lambda_b}^2}{q^2} \sum_i C_i \mathcal{H}_\perp^{(i)}(q^2) \equiv f_\perp(q^2) \left(C_9 + \Delta C_{9,\perp}(q^2) \right), \quad (2.11)$$

$$C_9 g_+(q^2) \rightarrow C_9 g_+(q^2) - 16\pi^2 \frac{2M_{\Lambda_b}^2}{q^2} \sum_i C_i \mathcal{H}_{+5}^{(i)}(q^2) \equiv g_+(q^2) \left(C_9 + \Delta C_{9,+5}(q^2) \right), \quad (2.12)$$

$$C_9 g_\perp(q^2) \rightarrow C_9 g_\perp(q^2) - 16\pi^2 \frac{2M_{\Lambda_b}^2}{q^2} \sum_i C_i \mathcal{H}_{\perp 5}^{(i)}(q^2) \equiv g_\perp(q^2) \left(C_9 + \Delta C_{9,\perp 5}(q^2) \right). \quad (2.13)$$

Similar relations are known for the mesonic counterpart $B \rightarrow K^{(*)} \ell^+ \ell^-$, see, for instance, refs. [28, 33].

2.3 Light-cone vectors and power counting

It is convenient to introduce the following light-cone vectors

$$\begin{aligned} n_+^\mu &\equiv \frac{(\sqrt{s_+} + \sqrt{s_-})^2}{2M_{\Lambda_b} \sqrt{s_+ s_-}} p^\mu - \frac{2M_{\Lambda_b}}{\sqrt{s_+ s_-}} p'^\mu, \\ n_-^\mu &\equiv -\frac{(\sqrt{s_+} - \sqrt{s_-})^2}{2M_{\Lambda_b} \sqrt{s_+ s_-}} p^\mu + \frac{2M_{\Lambda_b}}{\sqrt{s_+ s_-}} p'^\mu, \end{aligned} \quad (2.14)$$

such that

$$n_+^2 = n_-^2 = 0, \quad n_+ \cdot n_- = 2, \quad p^\mu = M_{\Lambda_b} \frac{n_+^\mu + n_-^\mu}{2} \equiv M_{\Lambda_b} v^\mu, \quad (2.15)$$

with v^μ being the four-velocity of the Λ_b baryon, and the transverse metric can simply be written as

$$g_\perp^{\mu\nu} = g^{\mu\nu} - \frac{n_+^\mu n_-^\nu + n_-^\mu n_+^\nu}{2}. \quad (2.16)$$

One can decompose any momentum vector in light-cone coordinates and consider the scaling of the individual momentum projections with a small expansion parameter $\lambda \ll 1$. In our case, we take

$$\lambda^2 \sim \frac{\Lambda_{\text{QCD}}}{m_b} \ll 1, \quad (2.17)$$

with $m_b \sim M_{\Lambda_b}$ being the mass of the heavy b -quark. To identify the power-counting of the various momenta, we use the short-hand notation

$$k^\mu : \{(n_+ \cdot k), k_\perp, (n_- \cdot k)\} \sim (\lambda^a, \lambda^b, \lambda^c), \quad (2.18)$$

where the powers of λ indicate the momentum scaling in units of m_b . For the b -quark, which is treated as a quasi-static colour source in the framework of heavy-quark effective theory (HQET), we thus have

$$\text{HQET } b\text{-quark : } p_b^\mu = m_b v^\mu + \Delta k^\mu, \quad \text{with } \Delta k^\mu \sim (\lambda^2, \lambda^2, \lambda^2), \quad (2.19)$$

and Δk^μ is referred to as a *soft* residual momentum. Similarly, the light quarks and gluons in the Λ_b bound state have soft momentum scaling:

$$\text{soft momenta in } \Lambda_b \text{ baryon : } k_s^\mu \sim (\lambda^2, \lambda^2, \lambda^2), \quad (2.20)$$

with virtualities $k_s^2 \sim \lambda^4$. In this work, we concentrate on the large-recoil region, where — in the rest frame of Λ_b — the energy of the hadronic final state is of the order $M_{\Lambda_b}/2$. The light constituents of the Λ have *collinear* momenta, scaling as

$$\text{collinear momenta in } \Lambda \text{ baryon : } k_c^\mu \sim (1, \lambda^2, \lambda^4), \quad (2.21)$$

with virtualities $k_c^2 \sim \lambda^4$. Interactions between field modes with soft and collinear momenta are induced by *hard-collinear* momenta,

$$\text{internal hard-collinear modes : } k_{\text{hc}}^\mu \sim (1, \lambda, \lambda^2) \quad (2.22)$$

with virtualities $k_{\text{hc}}^2 \sim \lambda^2$. Here, the scaling $k_{\text{hc}}^\perp \sim \lambda$ refers to hard-collinear modes in loops (while tree-level interactions would have $k_{\text{hc}}^\perp \sim \lambda^2$). Finally, the momentum transfer to the lepton pair is given by

$$q^\mu = (p - p')^\mu \sim (\lambda^2, 0, 1), \quad \text{with } q^2 \sim \lambda^2 \quad (\text{anti-hard-collinear}) \quad (2.23)$$

and is referred to as *anti-hard-collinear* (this excludes the kinematic limit $q^2 \rightarrow 0$).

3 Calculation of the “annihilation topologies”

3.1 Definition of the correlator

The first step in the derivation of the sum rule is the definition of a suitable correlator that allows the extraction of the required matrix element in (2.8). To this end, we replace the light baryon in the final state by an interpolating current,

$$J_\Lambda(y) \equiv \epsilon_{ijk} \left[u^{T,i}(y) C \gamma_5 \not{p}_+ d^j(y) \right] \frac{\not{p}_- \not{p}_+}{4} s^k(y), \quad (3.1)$$

for which we use the same expression as in ref. [21]. In particular, we use the projector $\frac{\not{p}_- \not{p}_+}{4}$ to project onto the leading spinor components for a collinear fermion. Here C is the charge conjugation matrix, the indices i, j, k are colour indices, and the quark field $u^{T,i}$ denotes the transpose in Dirac space of the field u^i . In the following, the appearance of the charge conjugation matrix is always understood in the chiral representation for Dirac matrices, where

$$C = i\gamma^2\gamma^0 = -C^{-1} = -C^T \quad (\text{chiral representation}),$$

and

$$C\gamma^\mu C^{-1} = -(\gamma^\mu)^T, \quad C\gamma_5 C^{-1} = (\gamma_5)^T.$$

With this, we define the correlator as

$$\Pi_\mu(n_- \cdot p') \equiv (i)^2 \int d^4x e^{iq \cdot x} \int d^4y e^{ip' \cdot y} \langle 0 | \mathcal{T} \left\{ J_\Lambda(y) \mathcal{O}_{3-6}(0) J_\mu^{\text{em}}(x) \right\} | \Lambda_b(p) \rangle. \quad (3.2)$$

Here we consider the correlator as a function of the *small* light-cone projection $n_- \cdot p'$ for a fixed value of the large light-cone projection

$$n_+ \cdot p' \simeq M_{\Lambda_b} - q^2/M_{\Lambda_b}. \quad (3.3)$$

As a consequence, the value of q^2 is determined by the value of $n_+ \cdot p'$ and vice versa. For the perturbative calculation of the correlator, we take the momentum associated to the interpolating current to be *hard-collinear*:

$$p' \sim (1, 0, \lambda^2), \quad \text{with } p'^2 = m_\Lambda^2 \sim \lambda^2 \quad (\text{hard-collinear}). \quad (3.4)$$

Note that the correlator has an open spinor index inherited from the strange-quark field in the interpolating current $J_\Lambda(y)$.

3.2 Hadronic representation of the correlator

To derive the hadronic dispersive representation of the correlator, we use unitarity, which consists in inserting a complete set of hadronic states between the interpolating current and the four-quark operators in eq. (3.2). We obtain

$$\begin{aligned} \Pi_\mu^{\text{had}}(n_- \cdot p') &= i \int d^4x e^{iq \cdot x} \sum_{s'} \frac{\langle 0 | J_\Lambda(0) | \Lambda(p', s') \rangle \langle \Lambda(p', s') | \mathcal{T} \{ \mathcal{O}_{3-6}(0) J_\mu^{\text{em}}(x) \} | \Lambda_b(p) \rangle}{m_\Lambda^2 - (p')^2} + \dots \\ &= \sum_{s'} \frac{\langle 0 | J_\Lambda(0) | \Lambda(p', s') \rangle \mathcal{H}_\mu^{(i)}}{m_\Lambda^2 - (p')^2} + \dots, \end{aligned} \quad (3.5)$$

where the ellipses denote the contribution of the continuum and excited states and we have used our definition of the non-local matrix elements in eq. (2.8). We define the decay constant of the Λ baryon as in ref. [21]:

$$\langle 0 | J_\Lambda(0) | \Lambda(p', s') \rangle = (n_+ \cdot p') f_\Lambda \frac{\not{n}_- \not{n}_+}{4} u_\Lambda(p', s'), \quad (3.6)$$

which implies that f_Λ has mass dimension 2. Using eq. (3.6) and the projections in eq. (2.9) yields

$$\begin{aligned} p^\mu \Pi_\mu^{\text{had}}(n_- \cdot p') &= - \frac{M_{\Lambda_b}^2 f_\Lambda (n_+ \cdot p' + m_\Lambda)(n_+ \cdot p') \not{n}_-}{2q^2 m_\Lambda^2 - (n_- \cdot p')(n_+ \cdot p')} \frac{\not{n}_-}{2} \\ &\quad \times \left[s_-(M_{\Lambda_b} + m_\Lambda) \mathcal{H}_+^{(i)}(q^2) - s_+(M_{\Lambda_b} - m_\Lambda) \mathcal{H}_{+5}(q^2) \gamma_5 \right] u_{\Lambda_b}(p) + \dots, \end{aligned} \quad (3.7)$$

$$\begin{aligned} g_\perp^{\mu\nu} \Pi_\mu^{\text{had}}(n_- \cdot p') &= M_{\Lambda_b}^2 \frac{f_\Lambda (n_+ \cdot p' - m_\Lambda)(n_+ \cdot p') \not{n}_-}{m_\Lambda^2 - (n_- \cdot p')(n_+ \cdot p')} \frac{\not{n}_-}{2} \\ &\quad \times \left[\mathcal{H}_\perp^{(i)}(q^2) \gamma_\perp^\nu - \mathcal{H}_{\perp 5}^{(i)}(q^2) \gamma_\perp^\nu \gamma_5 \right] u_{\Lambda_b}(p) + \dots \end{aligned} \quad (3.8)$$

Here in performing the spin summation, we have used that

$$\begin{aligned} \frac{\not{n}_- \not{n}_+}{4} (\not{p}' + m_\Lambda) u_{\Lambda_b}(p) &= ((n_+ \cdot p') + m_\Lambda) \frac{\not{n}_-}{2} u_{\Lambda_b}(p), \\ \frac{\not{n}_- \not{n}_+}{4} (\not{p}' + m_\Lambda) \gamma_\perp^\nu u_{\Lambda_b}(p) &= ((n_+ \cdot p') - m_\Lambda) \frac{\not{n}_-}{2} \gamma_\perp^\nu u_{\Lambda_b}(p) \end{aligned} \quad (3.9)$$

in our chosen reference frame with $p'_\perp = 0$ and $\frac{\not{n}_- \not{n}_+}{4} u_{\Lambda_b}(p) = \frac{\not{n}_-}{2} u_{\Lambda_b}(p)$.

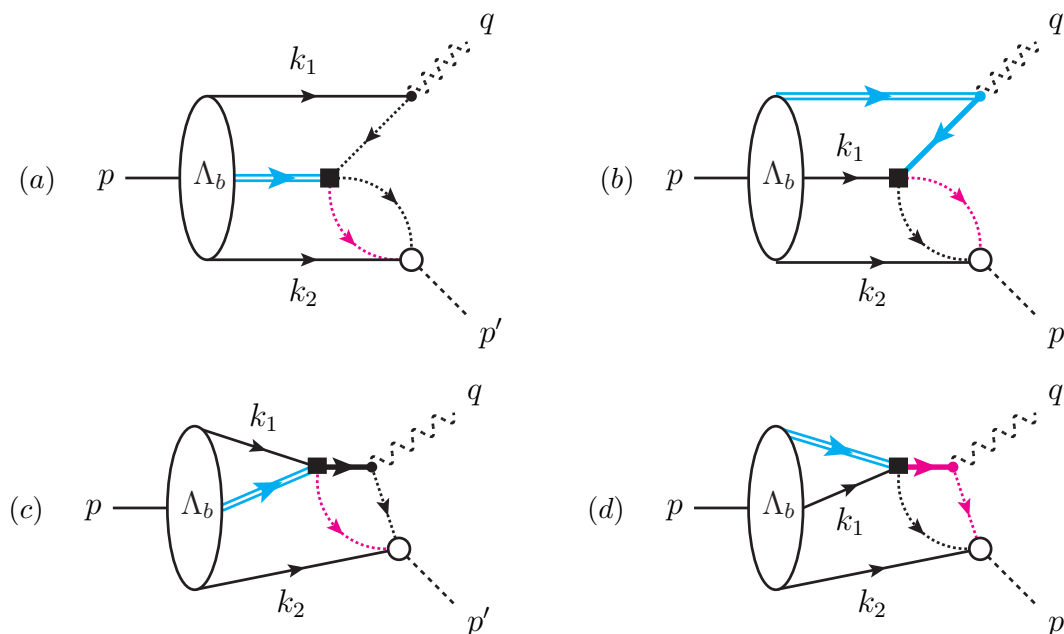


Figure 2. Leading-order annihilation diagrams contributing to the correlator in eq. (3.2). In each diagram, the lines labelled with momentum k_1 and k_2 should be identified with up- and down-quark, or vice versa. The b -quark is indicated by a light blue line; the strange quark by a magenta line. In addition, (anti-)hard-collinear propagators are indicated by dotted lines, and hard propagators by thick lines. The double line denotes the b -quark in HQET.

3.3 OPE analysis of the correlator

For the power counting defined in section 2.3, the correlator (3.2) can be calculated using an operator product expansion (OPE). At leading order in the strong coupling, and restricting ourselves to the “annihilation topologies”, the OPE analysis of the correlator corresponds to the four types of diagrams shown in figure 2. Each diagram comes in two copies, related by isospin symmetry, where the lines labelled by the momenta k_1 (and k_2) correspond to u (and d), or vice versa. Throughout we take the light quarks u, d, s to be massless. Notice that the diagram in which the photon is emitted from the spectator quark labelled by k_2 does *not* contribute to the discontinuity of $\Pi(n_- \cdot p')$ and can therefore be ignored.

In figure 2 we also indicate the virtuality of the internal propagators, which follows from the kinematics given above, together with a method-of-regions analysis of the loop integral. As can be seen, diagrams (b)-(d) all contain a *hard* quark propagator, in addition to a loop with two hard-collinear light-quark propagators. In contrast, diagram (a) contains an additional anti-hard-collinear propagator instead. This leads to an enhancement of diagram (a) compared to the other three diagrams. After integrating out the hard propagators, diagram (a) would thus match onto a correlator in SCET where the quark fields in QCD are trivially replaced by their SCET counterparts. On the other hand, in SCET diagrams (b)-(c) would correspond to another type of correlator in terms of an effective operator involving four quark fields and one additional photon field. In the following, we thus concentrate on diagram (a) since it is expected to give the highest power in the Λ/m_b expansion. Moreover, as we discuss in detail

below, the appearance of an anti-hard-collinear propagator together with a hard-collinear loop implies that the information about the configuration of the soft momenta k_1 and k_2 in the Λ_b bound state is contained in a new type of soft functions that requires a generalisation of the concept of LCDAs for the Λ_b . This makes diagram (a) particularly interesting from a conceptual point of view.

By inserting the effective operators and the currents into eq. (3.2), we obtain the following expression for diagram (a)

$$\begin{aligned} \Pi_\mu^{\text{OPE}}(n_- \cdot p') &= -Q_u \epsilon_{ijk} \int d^4x e^{iq \cdot x} \int d^4y e^{ip' \cdot y} \\ &\times \langle 0 | \mathcal{T} \left\{ \left[u^{T,i}(y) C \gamma_5 \not{n}_+ d^j(y) \right] \frac{\not{n}_- \not{n}_+}{4} s^k(y) \right. \\ &\quad \left. \times \left[\bar{s}^{l(m)} \gamma^\nu P_L b^l \right](0) \left[\bar{u}^{m(l)} \gamma_\nu P_{L(R)} u^m \right](0) \left[\bar{u}^n \gamma_\mu u^n \right](x) \right\} | \Lambda_b(p) \rangle, \end{aligned} \quad (3.10)$$

where colour indices are explicit, and spinor indices within square brackets are contracted. For concreteness, we have taken the case where the photon is emitted from the u quark. Due to the isospin symmetry, the case where the photon is emitted from the d quark gives the same result except for the replacement $Q_u \rightarrow Q_d$, since we neglect the light quark masses. The projector P_L (P_R) acting on the up quark field is for the case of \mathcal{O}_3 and \mathcal{O}_4 (\mathcal{O}_5 and \mathcal{O}_6) operators. In addition, the colour indices without (with) parenthesis refer to the case of \mathcal{O}_3 and \mathcal{O}_5 (\mathcal{O}_4 and \mathcal{O}_6) operators, respectively.

Performing the Wick contractions corresponding to the diagram figure 2(a), we get

$$\begin{aligned} \Pi_\mu^{\text{OPE}}(n_- \cdot p') &= -Q_u \epsilon_{ijk} \delta^{im(il)} \delta^{kl(km)} \int d^4x e^{iq \cdot x} \int d^4y e^{ip' \cdot y} \\ &\langle 0 | \left[d^{T,j}(y) C \gamma_5 \not{n}_+ S_F^{(u)}(y) \gamma_\nu P_{L(R)} S_F^{(u)}(-x) \gamma_\mu u^m(x) \right] \left[\frac{\not{n}_- \not{n}_+}{4} S_F^{(s)}(y) \gamma^\nu P_L b^l(0) \right] | \Lambda_b(p) \rangle, \end{aligned} \quad (3.11)$$

where the fermion propagators S_F is defined as

$$S_F(x-y) \equiv \langle 0 | \mathcal{T} \psi(x) \bar{\psi}(y) | 0 \rangle = i \int \frac{d^4p}{(2\pi)^4} \frac{\not{p} + m}{p^2 - m^2 + i\epsilon} e^{-ip \cdot (x-y)}. \quad (3.12)$$

Realising that the alternative colour contractions in brackets only yield an extra minus sign and performing the trivial integrations of the space-time coordinates, eq. (3.11) can be written as

$$\begin{aligned} \Pi_\mu^{\text{OPE}}(n_- \cdot p') &= \pm i Q_u \epsilon_{ijk} \int \frac{d^4\ell_2}{(2\pi)^4} \int \frac{d^4k_1}{(2\pi)^4} \int \frac{d^4k_2}{(2\pi)^4} \\ &\times \langle 0 | \left[\bar{d}^{T,j}(k_2) C \gamma_5 \not{n}_+ \frac{\not{\ell}_2}{\ell_2^2 + i\epsilon} \gamma_\nu P_{L(R)} \frac{\not{k}_1 - \not{q}}{(k_1 - q)^2 + i\epsilon} \gamma_\mu \tilde{u}^i(k_1) \right] \\ &\times \left[\frac{\not{n}_- \not{n}_+}{4} \frac{\not{p}' - \not{\ell}_2 - \not{k}_2}{(p' - \ell_2 - k_2)^2 + i\epsilon} \gamma^\nu P_L b^k(0) \right] | \Lambda_b(p) \rangle, \end{aligned} \quad (3.13)$$

where we denoted the Fourier transformed quark fields with a tilde.

At this step, we perform the tensor reduction for the integration over the loop momentum ℓ_2 . We define

$$T^{\alpha\beta} = \int [d\ell_2] \frac{\ell_2^\alpha (q' - \ell_2)^\beta}{(\ell_2^2 + i\epsilon)((q' - \ell_2)^2 + i\epsilon)} = A(q'^2) g^{\alpha\beta} + B(q'^2) \frac{q'^\alpha q'^\beta}{q'^2} \quad (3.14)$$

with $q' = p' - k_2$ and — for the moment — consider the loop integration in $D \neq 4$ dimensions, such that

$$[d\ell_2] \equiv i \mu^{4-D} \frac{d^D \ell_2}{(2\pi)^D}.$$

Since the LCSRs are derived using a dispersion relation of the form

$$\Pi_\mu^{\text{OPE}}(n_- \cdot p') = \frac{1}{\pi} \int_0^\infty ds \frac{\text{Im} \Pi_\mu^{\text{OPE}}(s/(n_+ \cdot p'))}{s - (n_+ \cdot p')(n_- \cdot p') - i\epsilon}, \quad n_+ \cdot p' > 0, \quad (3.15)$$

we only need the discontinuity of the correlator. Thus, only the imaginary part of the integrals $A(s)$ and $B(s)$ is relevant in our calculation, which is finite for $D \rightarrow 4$. Performing the algebra, we have

$$A(q'^2) = \frac{1}{D-1} \frac{1}{q'^2} \int [d\ell_2] \frac{(q' \cdot \ell_2)^2 - \ell_2^2 q'^2}{(\ell_2^2 + i\epsilon)((q' - \ell_2)^2 + i\epsilon)}, \quad (3.16)$$

$$B(q'^2) = \frac{1}{q'^2} \int [d\ell_2] \frac{(q'^2 - (\ell_2 \cdot q'))(\ell_2 \cdot q')}{(\ell_2^2 + i\epsilon)((q' - \ell_2)^2 + i\epsilon)} - A(q'^2). \quad (3.17)$$

The imaginary part of these integrals is then easily calculated:

$$\text{Im} A(s) = -\frac{s \theta[s]}{192\pi}, \quad \text{Im} B(s) = -\frac{s \theta[s]}{96\pi}. \quad (3.18)$$

Inserting these results in eq. (3.13), we obtain

$$\begin{aligned} \text{Im} \Pi_\mu^{\text{OPE}}(n_- \cdot p') &= \mp \frac{Q_u \epsilon_{ijk}}{192\pi} \int \frac{d^4 k_1}{(2\pi)^4} \int \frac{d^4 k_2}{(2\pi)^4} \theta((p' - k_2)^2) \\ &\quad \times \left\{ g^{\alpha\beta} (p' - k_2)^2 + 2 (p' - k_2)^\alpha (p' - k_2)^\beta \right\} \\ &\quad \times \langle 0 | \left[\tilde{d}^{T,j}(k_2) C \gamma_5 \not{p}_+ \gamma_\alpha \gamma_\nu P_{L(R)} \frac{\not{k}_1 - \not{q}}{(k_1 - q)^2 + i\epsilon} \gamma_\mu \tilde{u}^i(k_1) \right] \\ &\quad \times \left[\frac{\not{p}_- \not{p}_+}{4} \gamma_\beta \gamma^\nu P_L b^k(0) \right] | \Lambda_b(p) \rangle. \end{aligned} \quad (3.19)$$

We observe that at leading power in the expansion parameter λ , the above expression depends on two *opposite* light-cone projections of the light-quark momenta in the Λ_b baryon. The integrals over the loop momentum ℓ_2 depend on

$$(p' - k_2)^2 \simeq (n_+ \cdot p')(n_- \cdot p' - n_- \cdot k_2) \sim \lambda^2,$$

while the remaining light-quark propagator connecting the external photon and the effective four-quark operator depends on

$$(k_1 - q)^2 \simeq (n_- \cdot q)(n_+ \cdot q - n_+ \cdot k_1) \sim \lambda^2.$$

In the SCET jargon, the associated short-distance dynamics is described by *hard-collinear* modes, but in different light-cone directions (one in the direction of p' , and the other in the direction of q). After performing a Fourier transform to position space, this would correspond to tri-local matrix elements of the form

$$\langle 0 | d_{\beta}^j(\tau_2 n_-) u_{\alpha}^i(\tau_1 n_+) b_{\delta}^k(0) | \Lambda_b(p) \rangle,$$

where we have made the spinor indices α, β, δ explicit. These objects define a new type of three-particle LCDAs or, more appropriately, “soft functions” in the context of SCET factorisation (for this, the light-quark fields have to be supplemented with the corresponding soft Wilson lines to render the tri-local operator gauge invariant). Their appearance in the “annihilation topologies” is due to the fact that the two quarks take part in different dynamics: one, associated to the interaction with an anti-collinear photon; and another, associated with the collinear momentum of the interpolating current.² Before proceeding with the sum rule, we discuss and classify the new type of soft functions and the connection with the conventional baryon LCDAs.

3.4 Λ_b soft functions with two light-like separations

The standard definitions of three-particle LCDAs for the Λ_b baryon can be found in ref. [40]. In order to generalise these definitions to our case, it is convenient to follow the procedure of ref. [41], where the starting point is the decomposition of the hadronic matrix element of a general tri-local operator:

$$\begin{aligned} & \epsilon_{ijk} \langle 0 | \left(u_{\alpha}^i(z_1) d_{\beta}^j(z_2) \right) b_{\delta}^k(0) | \Lambda_b(p) \rangle \\ & \equiv \frac{1}{4} \left\{ f_{\Lambda_b}^{(1)} \left[\tilde{M}^{(1)}(v, z_1, z_2) \gamma_5 C^{-1} \right]_{\beta\alpha} + f_{\Lambda_b}^{(2)} \left[\tilde{M}^{(2)}(v, z_1, z_2) \gamma_5 C^{-1} \right]_{\beta\alpha} \right\} u_{\Lambda_b, \delta}(v). \end{aligned} \quad (3.20)$$

Here z_1 and z_2 are space-time points and QCD gauge-links are understood implicitly. The Dirac matrices $\tilde{M}^{(1(2))}$ contain an even (odd) number of Dirac matrices, respectively. In the following, we focus on the matrix $\tilde{M}^{(2)}$ which is relevant for our sum rule. (The matrix $\tilde{M}^{(1)}$ can be treated in a completely analogous way, see ref. [41].) Here, the most general Lorentz-covariant decomposition is

$$\begin{aligned} \tilde{M}^{(2)}(v, z_1, z_2) &= \psi \tilde{\Phi}_2(t_1, t_2, z_1^2, z_2^2, z_1 \cdot z_2) + \frac{\tilde{\Phi}_X(t_1, t_2, z_1^2, z_2^2, z_1 \cdot z_2)}{4t_1 t_2} (\not{z}_2 \psi \not{z}_1 - \not{z}_1 \psi \not{z}_2) \\ &+ \frac{\tilde{\Phi}_{42}^{(i)}(t_1, t_2, z_1^2, z_2^2, z_1 \cdot z_2)}{2t_1} \not{z}_1 + \frac{\tilde{\Phi}_{42}^{(ii)}(t_1, t_2, z_1^2, z_2^2, z_1 \cdot z_2)}{2t_2} \not{z}_2, \end{aligned} \quad (3.21)$$

where $t_i = v \cdot z_i$. The standard LCDAs can be obtained by expanding the above expression around the limit $z_1^2 = z_2^2 = z_1 \cdot z_2 = 0$. However, for the new type of soft functions, we rather have to consider the expansion for the situation $n_+ \cdot z_1 \ll z_1^{\perp} \ll n_- \cdot z_1$ and $n_- \cdot z_2 \ll z_2^{\perp} \ll n_+ \cdot z_2$, such that $t_1 \approx \bar{\tau}_1 = \frac{n_- \cdot z_1}{2}$, $t_1 \approx \tau_2 = \frac{n_+ \cdot z_2}{2}$, and $z_1 \cdot z_2 \approx 2\bar{\tau}_1 \tau_2$.

²The appearance of soft b -hadron matrix elements with two light-like separations has already been observed in other contexts, see e.g. refs. [34–39].

This yields

$$\begin{aligned}
 \tilde{M}^{(2)}(v, z_1, z_2) &\longrightarrow \frac{\not{n}_+}{2} \left(\tilde{\chi}_2(\bar{\tau}_1, \tau_2) + \tilde{\chi}_{42}^{(i)}(\bar{\tau}_1, \tau_2) \right) + \frac{\not{n}_-}{2} \left(\tilde{\chi}_2(\bar{\tau}_1, \tau_2) + \tilde{\chi}_{42}^{(ii)}(\bar{\tau}_1, \tau_2) \right) \\
 &+ \frac{\tilde{\chi}_{42}^{(i)}(\bar{\tau}_1, \tau_2)}{2\bar{\tau}_1} \not{z}_1^\perp + \frac{\tilde{\chi}_{42}^{(ii)}(\bar{\tau}_1, \tau_2)}{2\tau_2} \not{z}_2^\perp \\
 &+ \tilde{\chi}_X(\bar{\tau}_1, \tau_2) \left(\frac{\not{z}_1^\perp}{2\bar{\tau}_1} + \frac{\not{z}_2^\perp}{2\tau_2} \right) \left(\frac{\not{n}_- \not{n}_+}{4} - \frac{\not{n}_+ \not{n}_-}{4} \right) + \mathcal{O}(z_{i\perp}^2, n_- \cdot z_2, n_+ \cdot z_1),
 \end{aligned} \tag{3.22}$$

where $\bar{\tau}_1 = n_- \cdot z_1/2$ and $\tau_2 = n_+ \cdot z_2/2$, and

$$\tilde{\chi}_2(\bar{\tau}_1, \tau_2) = \tilde{\Phi}_2(\bar{\tau}_1, \tau_2, 0, 0, 2\bar{\tau}_1\tau_2) \quad \text{etc.}$$

This should be compared with the standard LCDAs, which are given by

$$\tilde{\phi}_2(\tau_1, \tau_2) = \tilde{\Phi}_2(\tau_1, \tau_2, 0, 0, 0) \quad \text{etc.}$$

We introduce the LCDAs in momentum space by performing a Fourier transform

$$\chi(\bar{\omega}_1, \omega_2) \equiv \int_{-\infty}^{\infty} \frac{d\bar{\tau}_1}{2\pi} e^{i\bar{\omega}_1\bar{\tau}_1} \int_{-\infty}^{\infty} \frac{d\tau_2}{2\pi} e^{i\omega_2\tau_2} \tilde{\chi}(\bar{\tau}_1, \tau_2) \tag{3.23}$$

Therefore, from the Fourier transform of eq. (3.22), we can construct the momentum-space projector:

$$\begin{aligned}
 M^{(2)}(\bar{\omega}_1, \omega_2) &= \frac{\not{n}_+}{2} \left(\chi_2(\bar{\omega}_1, \omega_2) + \chi_{42}^{(i)}(\bar{\omega}_1, \omega_2) \right) \\
 &+ \frac{\not{n}_-}{2} \left(\chi_2(\bar{\omega}_1, \omega_2) + \chi_{42}^{(ii)}(\bar{\omega}_1, \omega_2) \right) \\
 &- \frac{1}{2} \gamma_\rho^\perp \left(\bar{\chi}_{42}^{(i)}(\bar{\omega}_1, \omega_2) - \bar{\chi}_X(\bar{\omega}_1, \omega_2) \right) \frac{\not{n}_+ \not{n}_-}{4} \frac{\partial}{\partial k_{1\rho}^\perp} \\
 &- \frac{1}{2} \gamma_\rho^\perp \left(\bar{\chi}_{42}^{(ii)}(\bar{\omega}_1, \omega_2) + \bar{\chi}_X(\bar{\omega}_1, \omega_2) \right) \frac{\not{n}_- \not{n}_+}{4} \frac{\partial}{\partial k_{1\rho}^\perp} \\
 &- \frac{1}{2} \gamma_\rho^\perp \left(\hat{\chi}_{42}^{(ii)}(\bar{\omega}_1, \omega_2) + \hat{\chi}_X(\bar{\omega}_1, \omega_2) \right) \frac{\not{n}_- \not{n}_+}{4} \frac{\partial}{\partial k_{2\rho}^\perp} \\
 &- \frac{1}{2} \gamma_\rho^\perp \left(\hat{\chi}_{42}^{(i)}(\bar{\omega}_1, \omega_2) - \hat{\chi}_X(\bar{\omega}_1, \omega_2) \right) \frac{\not{n}_+ \not{n}_-}{4} \frac{\partial}{\partial k_{2\rho}^\perp},
 \end{aligned} \tag{3.24}$$

where the derivatives are understood to act on a hard-scattering kernel that has been Taylor-expanded in transverse momenta, and we define

$$\bar{\omega}_1 = n_+ \cdot k_1, \quad \omega_2 = n_- \cdot k_2. \tag{3.25}$$

We also introduced the abbreviations

$$\begin{aligned}
 \bar{\chi}(\bar{\omega}_1, \omega_2) &\equiv \int_0^{\bar{\omega}_1} d\bar{\eta}_1 \chi(\bar{\eta}_1, \omega_2), \\
 \hat{\chi}(\bar{\omega}_1, \omega_2) &\equiv \int_0^{\omega_2} d\eta_2 \chi(\bar{\omega}_1, \eta_2).
 \end{aligned} \tag{3.26}$$

Explicit models for these LCDAs are derived in appendix A.

3.5 Expressing the correlator in terms of soft functions

We can now proceed to express the hadronic matrix element appearing in the leading order result for the correlator (3.19) in terms of the momentum-space projector following from (3.20) and (3.24). To this end, we write the hadronic matrix element in eq. (3.19) as a Dirac trace:

$$\begin{aligned}
 & \int \frac{d^4 k_1}{(2\pi)^4} \int \frac{d^4 k_2}{(2\pi)^4} \epsilon_{ijk} \langle 0 | [\tilde{d}^{T,j}(k_2) \Gamma \tilde{u}^i(k_1)] b^k(0) | \Lambda_b(p) \rangle f^{\alpha\beta}(k_2^\perp) \\
 &= - \int \frac{d^4 k_1}{(2\pi)^4} \int \frac{d^4 k_2}{(2\pi)^4} \epsilon_{ijk} \langle 0 | [\tilde{u}^{T,i}(k_1) \Gamma^T \tilde{d}^j(k_2)] b^k(0) | \Lambda_b(p) \rangle f^{\alpha\beta}(k_2^\perp) \\
 &= - \frac{1}{4} f_{\Lambda_b}^{(2)} \int_0^\infty d\bar{\omega}_1 \int_0^\infty d\omega_2 \text{tr}[M^{(2)}(\bar{\omega}_1, \omega_2) \gamma_5 C^{-1} \Gamma^T] f^{\alpha\beta}(k_2^\perp) u_{\Lambda_b}(v) \Big|_{k_i^\perp=0}, \quad (3.27)
 \end{aligned}$$

with

$$\Gamma = C \gamma_5 \not{k}_+ \gamma_\alpha \gamma_\nu P_{L(R)} (\not{k}_1 - \not{q}) \gamma_\mu \quad (3.28)$$

and hence

$$\Gamma^T = C \gamma_\mu (\not{k}_1 - \not{q}) P_{L(R)} \gamma_\nu \gamma_\alpha \not{k}_+ \gamma_5. \quad (3.29)$$

The function $f^{\alpha\beta}(k_2^\perp)$ can be read off eq. (3.19):

$$\begin{aligned}
 f^{\alpha\beta}(k_2^\perp) &\equiv g^{\alpha\beta} (p' - k_2)^2 + 2 (p' - k_2)^\alpha (p' - k_2)^\beta \\
 &= \frac{(n_+ \cdot p')^2}{2} n_-^\alpha n_-^\beta + (n_+ \cdot p') (n_- \cdot p' - n_- \cdot k_2) g_\perp^{\alpha\beta} \\
 &\quad - (n_+ \cdot p') n_-^\alpha (k_2^\perp)^\beta - (n_+ \cdot p') n_-^\beta (k_2^\perp)^\alpha + \mathcal{O}(\lambda^4), \quad (3.30)
 \end{aligned}$$

where we have kept terms of order λ^2 but dropped subsubleading terms of order λ^4 , as well as terms proportional to n_+^α or n_+^β which do not contribute in (3.19). To derive eq. (3.29) we have used that $\gamma_\mu^T = -C \gamma^\mu C^{-1}$, and the additional sign in front of the trace stems from anti-commuting the field operators $u_\alpha(z_1)$ and $d_\beta(z_2)$ when using eq. (3.20) in (3.19). As already mentioned, the projector $M^{(1)}$ does not contribute to the trace, because the Dirac structure Γ has an odd number of Dirac matrices. For later convenience, we also expand the term $(\not{k}_1 - \not{q})$ up to $\mathcal{O}(\lambda^4)$:

$$\not{k}_1 - \not{q} = -(n_- \cdot q) \frac{\not{k}_+}{2} + \not{k}_1^\perp + \frac{\not{k}_+}{2} (n_- \cdot k_1) + \frac{\not{k}_-}{2} (\bar{\omega}_1 - n_+ \cdot q) + \mathcal{O}(\lambda^4). \quad (3.31)$$

Let us first consider the contribution arising from the leading term in $f^{\alpha\beta}$ together with the leading term in $(\not{k}_1 - \not{q})$. For this we obtain

$$\begin{aligned}
 & - \frac{1}{4} \text{tr}[M^{(2)} \gamma_5 C^{-1} \Gamma^T] f^{\alpha\beta}(k_2^\perp) \Big|_{k_i^\perp=0, \text{ leading}} \\
 &= (n_- \cdot q) (n_+ \cdot p')^2 n_-^\beta \left(- \frac{g_{\mu\nu}^\perp}{2} \pm \frac{i \epsilon_{\mu\nu\{n_-\}\{n_+\}}}{4} \right) \left(\chi_2(\bar{\omega}_1, \omega_2) + \chi_{42}^{(ii)}(\bar{\omega}_1, \omega_2) \right), \quad (3.32)
 \end{aligned}$$

where the upper sign is for the operators $\mathcal{O}_{3,4}$, and the lower sign for $\mathcal{O}_{5,6}$. For the Levi-Civita symbol we use the convention $\epsilon^{0123} = 1$ and the short-hand notation $\epsilon_{\mu\nu\rho\sigma} q^\sigma \equiv \epsilon_{\mu\nu\rho\{q\}}$. Note that eq. (3.32) fixes the Lorentz index μ to be transversal and hence this term only contributes to the LCSR for $\mathcal{H}_{\perp(5)}^{(i)}$. We can now easily obtain the leading contribution to the OPE calculation of $\text{Im } \Pi_{\mu}^{\text{OPE}}$ by plugging eqs. (3.27) and (3.32) into eq. (3.19):

$$\begin{aligned} \text{Im } \Pi_{\mu}^{\text{OPE}}(n_{-} \cdot p') &= \mp \frac{Q_u f_{\Lambda_b}^{(2)}}{192\pi} (n_{+} \cdot p')^2 \\ &\times \int_0^{\infty} d\bar{\omega}_1 \int_0^{\infty} d\omega_2 \frac{\theta(n_{-} \cdot p' - \omega_2)}{n_{+} \cdot q - \bar{\omega}_1 + i\epsilon} \left(\chi_2(\bar{\omega}_1, \omega_2) + \chi_{42}^{(ii)}(\bar{\omega}_1, \omega_2) \right) \\ &\times \left(-\frac{g_{\mu\nu}^{\perp}}{2} \pm \frac{i\epsilon_{\mu\nu\{n_{-}\}\{n_{+}\}}}{4} \right) [\not{n}_{-} \gamma_{\perp}^{\nu} P_L] u_{\Lambda_b}(v) + \mathcal{O}(\lambda^2). \end{aligned} \quad (3.33)$$

This can be further simplified by using that after combining with the Dirac projection of the b -quark field in (3.19), we have

$$\left(-\frac{g_{\mu\nu}^{\perp}}{2} + \frac{i\epsilon_{\mu\nu\{n_{-}\}\{n_{+}\}}}{4} \right) [\not{n}_{-} \gamma_{\perp}^{\nu} P_L] = 0, \quad (3.34)$$

$$\left(-\frac{g_{\mu\nu}^{\perp}}{2} - \frac{i\epsilon_{\mu\nu\{n_{-}\}\{n_{+}\}}}{4} \right) [\not{n}_{-} \gamma_{\perp}^{\nu} P_L] = -\not{n}_{-} \gamma_{\mu}^{\perp} P_L, \quad (3.35)$$

which holds in $D = 4$ dimensions. Therefore only the operators \mathcal{O}_5 and \mathcal{O}_6 contribute to the LCSR for $\mathcal{H}_{\perp(5)}^{(i)}$ in the considered order of the calculation.

Actually, this result can already be understood by considering the Dirac structure of the original four-quark operators in QCD and projecting the light-quark fields onto the leading collinear or anti-collinear spinor components in SCET that correspond to the topology in figure 2(a). Ignoring the colour indices for the moment, one has by virtue of eqs. (3.34) and (3.35)

$$\left(\bar{s} \frac{\not{n}_{+} \not{n}_{-}}{4} \gamma^{\nu} P_L b \right) \left(\bar{q} \frac{\not{n}_{+} \not{n}_{-}}{4} \gamma_{\nu} P_L \frac{\not{n}_{+} \not{n}_{-}}{4} q \right) = 0, \quad (3.36)$$

$$\left(\bar{s} \frac{\not{n}_{+} \not{n}_{-}}{4} \gamma^{\nu} P_L b \right) \left(\bar{q} \frac{\not{n}_{+} \not{n}_{-}}{4} \gamma_{\nu} P_R \frac{\not{n}_{+} \not{n}_{-}}{4} q \right) = \left(\bar{s} \frac{\not{n}_{+} \not{n}_{-}}{4} \gamma_{\perp}^{\nu} P_L b \right) \left(\bar{q} \gamma_{\nu}^{\perp} P_R q \right). \quad (3.37)$$

It follows from this argument, that neither the current-current operators $\mathcal{O}_1^{(u)}$ and $\mathcal{O}_2^{(u)}$ — which have larger Wilson coefficients, but enter with Cabibbo-suppressed CKM factors in $b \rightarrow s$ transitions — contribute to the baryonic annihilation topologies at leading power. It is worth noting that in the mesonic counterpart, the role of \bar{q} and q is interchanged in the leading annihilation topology compared to the baryonic case; and for that reason — by the same argument — only the operators \mathcal{O}_3 and \mathcal{O}_4 (and also $\mathcal{O}_1^{(u)}$ and $\mathcal{O}_2^{(u)}$) contribute at leading power [9].

To proceed in the calculation of the associated non-local form factors $\mathcal{H}_{+}^{(i)}$, we contract eq. (3.27) with p^{μ} . Since the leading term vanishes, we consider sub-leading terms of $\mathcal{O}(\lambda^2)$:

$$\begin{aligned} &-\frac{1}{4} p^{\mu} \text{tr}[M^{(2)} \gamma_5 C^{-1} \Gamma^T] f^{\alpha\beta}(k_2^{\perp}) \Big|_{k_i^{\perp}=0, \text{ subleading}} \\ &= -\frac{1}{4} M_{\Lambda_b}(n_{+} \cdot p')(n_{-} \cdot q) \left(\hat{\chi}_{42}^{(ii)}(\bar{\omega}_1, \omega_2) + \hat{\chi}_X(\bar{\omega}_1, \omega_2) \right) \left(3n_{-}^{\beta} n_{+}^{\nu} - 2g^{\beta\nu} \mp i\epsilon^{\beta\nu\{n_{+}\}\{n_{-}\}} \right), \end{aligned} \quad (3.38)$$

where the terms proportional to $n_-^\beta n_-^\nu$ and n_+^β have been dropped, since they vanish once contracted with the Dirac matrix in the last line of eq. (3.19). We obtain the leading contribution to the OPE calculation of $p^\mu \text{Im} \Pi_\mu^{\text{OPE}}$ by inserting eqs. (3.27) and (3.38) into eq. (3.19) contracted with p^μ :

$$\begin{aligned}
 p^\mu \text{Im} \Pi_\mu^{\text{OPE}}(n_- \cdot p') &= \pm \frac{1}{4} \frac{Q_u f_{\Lambda_b}^{(2)}}{192\pi} M_{\Lambda_b}(n_+ \cdot p') \\
 &\times \int_0^\infty d\bar{\omega}_1 \int_0^\infty d\omega_2 \frac{\theta(n_- \cdot p' - \omega_2)}{n_+ \cdot q - \bar{\omega}_1 + i\epsilon} \left(\hat{\chi}_{42}^{(ii)}(\bar{\omega}_1, \omega_2) + \hat{\chi}_X(\bar{\omega}_1, \omega_2) \right) \\
 &\times [\gamma_\beta \not{p}_-] \left(\frac{g_\perp^{\beta\nu}}{2} \pm \frac{i\epsilon^{\beta\nu\{n_+\}\{n_-\}}}{4} \right) [\not{p}_+ \gamma_\nu P_L] u_{\Lambda_b}(v) + \mathcal{O}(\lambda^4), \quad (3.39)
 \end{aligned}$$

where we have used that

$$[\gamma_\beta \not{p}_-] \left(\frac{g_\perp^{\beta\nu}}{2} - \frac{i\epsilon^{\beta\nu\{n_+\}\{n_-\}}}{4} \right) [\not{p}_+ \gamma_\nu P_L] = 0 \quad (3.40)$$

$$[\gamma_\beta \not{p}_-] \left(\frac{g_\perp^{\beta\nu}}{2} + \frac{i\epsilon^{\beta\nu\{n_+\}\{n_-\}}}{4} \right) [\not{p}_+ \gamma_\nu P_L] u_{\Lambda_b}(v) = 8 \left[\frac{\not{p}_- \not{p}_+ P_L}{4} \right] u_{\Lambda_b}(v) = 8 \left[\frac{\not{p}_- P_R}{2} \right] u_{\Lambda_b}(v). \quad (3.41)$$

Therefore, in analogy with $\mathcal{H}_{\perp(5)}^{(i)}$ and as a consequence of eqs. (3.36) and (3.37), only the operators \mathcal{O}_5 and \mathcal{O}_6 contribute to the LCSR for $\mathcal{H}_{+(5)}^{(i)}$.

3.6 Derivation of light-cone sum rules

Following the usual procedure to derive a LCSR — see e.g. ref. [42] — we match the OPE calculation of the correlator Π_μ of eqs. (3.33) and (3.39) onto the corresponding hadronic representations of eqs. (3.7) and (3.8). The contribution of the continuum and excited states is removed by using the semi-global quark-hadron duality approximation. In practice, we assume that the second line of eqs. (3.7)–(3.8) is equal to the dispersive integral in the OPE calculation above the effective threshold s_0 , whose value is discussed in section 4. We perform a Borel transform with respect to the variable $(n_- \cdot p')$ to further suppress the continuum and excited states contribution. This reduces the systematic error due to the quark-hadron duality approximation. Performing a Borel transform in our case consists in replacing

$$\frac{1}{\mathcal{K} - n_- \cdot p'} \rightarrow e^{-\frac{\mathcal{K}}{\omega_M}}, \quad (3.42)$$

where ω_M is the associated Borel parameter and \mathcal{K} does not depend on $(n_- \cdot p')$. The bulky formulae resulting from the OPE calculation with the hadronic representation are collected in appendix B. In our calculation, this matching implies that (taking into account eqs. (3.34), (3.35)), (3.40), and (3.41))

$$\begin{aligned}
 \mathcal{H}_{\perp(5)}^{(5)} &= -\mathcal{H}_{\perp(5)}^{(6)}, \quad \mathcal{H}_{\perp(5)}^{(3)} = \mathcal{H}_{\perp(5)}^{(4)} = 0, \quad \mathcal{H}_\perp^{(i)} = \mathcal{H}_{\perp 5}^{(i)}, \\
 \mathcal{H}_{+(5)}^{(5)} &= -\mathcal{H}_{+(5)}^{(6)}, \quad \mathcal{H}_{+(5)}^{(3)} = \mathcal{H}_{+(5)}^{(4)} = 0, \quad \mathcal{H}_+^{(i)} = -\frac{s_+(M_{\Lambda_b} - m_\Lambda)}{s_-(M_{\Lambda_b} + m_\Lambda)} \mathcal{H}_{+5}^{(i)}, \quad (3.43)
 \end{aligned}$$

up to higher order corrections. Hence, in the limit $M_{\Lambda_b} \gg m_\Lambda$, the last of these identities becomes $\mathcal{H}_+^{(i)} = -\mathcal{H}_{+5}^{(i)}$. Thus, it is sufficient to present the LCSRs for, e.g., only $\mathcal{H}_\perp^{(5)}$ and $\mathcal{H}_+^{(5)}$. These LCSRs read

$$\begin{aligned} \mathcal{H}_\perp^{(5)}(q^2) &= \frac{f_{\Lambda_b}^{(2)}(Q_u + Q_d)}{f_\Lambda} \frac{1}{192\pi^2} \frac{1}{M_{\Lambda_b}^2(n_+ \cdot p' - m_\Lambda)} \\ &\times \int_0^{\sigma_0} d\sigma \int_0^\sigma d\omega_2 \int_0^\infty d\bar{\omega}_1 \frac{(n_+ \cdot p')^2}{n_+ \cdot q - \bar{\omega}_1 + i\epsilon} \left(\chi_2(\bar{\omega}_1, \omega_2) + \chi_{42}^{(ii)}(\bar{\omega}_1, \omega_2) \right) e^{\frac{m_\Lambda^2/(n_+ \cdot p') - \sigma}{\omega_M}}, \end{aligned} \quad (3.44)$$

and

$$\begin{aligned} \mathcal{H}_+^{(5)}(q^2) &= -\frac{f_{\Lambda_b}^{(2)}(Q_u + Q_d)}{f_\Lambda} \frac{q^2}{192\pi} \frac{1}{M_{\Lambda_b}(n_+ \cdot p' + m_\Lambda)} \frac{1}{s_-(M_{\Lambda_b} + m_\Lambda)} \\ &\times \int_0^{\sigma_0} d\sigma \int_0^\sigma d\omega_2 \int_0^\infty d\bar{\omega}_1 \frac{n_+ \cdot p'}{n_+ \cdot q - \bar{\omega}_1 + i\epsilon} \left(\hat{\chi}_{42}^{(ii)}(\bar{\omega}_1, \omega_2) + \hat{\chi}_X(\bar{\omega}_1, \omega_2) \right) e^{\frac{m_\Lambda^2/(n_+ \cdot p') - \sigma}{\omega_M}}, \end{aligned} \quad (3.45)$$

where $\sigma_{(0)} \equiv s_{(0)}/(n_+ \cdot p')$. The integrals can be performed analytically, assuming the models for the LCDAs given in appendix A. These formulae are given in appendix B.

The LCSRs for the non-local form factors $\mathcal{H}_{\perp(5)}^{(i)}$ and $\mathcal{H}_{+(5)}^{(i)}$ can be compared with the LCSR for the local form factor ξ_Λ derived in ref. [21]. In the large recoil limit, i.e. $(n_+ \cdot p') \sim M_{\Lambda_b}$, ξ_Λ is equal to each of the helicity form factors:

$$\xi_\Lambda(q^2) \simeq f_0(q^2) \simeq f_+(q^2) \simeq f_\perp(q^2) \simeq g_0(q^2) \simeq g_+(q^2) \simeq g_\perp(q^2). \quad (3.46)$$

The LCSR for ξ_Λ reads

$$\xi_\Lambda(q^2) = \frac{f_{\Lambda_b}^{(2)}}{f_\Lambda} \frac{1}{(n_+ \cdot p')} \int_0^{\sigma_0} d\sigma \phi_4(\sigma) e^{\frac{m_\Lambda^2/(n_+ \cdot p') - \sigma}{\omega_M}}, \quad (3.47)$$

where ϕ_4 is one the standard LCDAs partially integrated (see ref. [21] for its definition). Comparing this sum rule with the one for $\mathcal{H}_\perp^{(5)}$, we observe that they contribute at the same power of λ^2 . The factor of 192π due to the loop in eq. (3.44) is compensated in the decay amplitude by the factor $-16\pi^2 \frac{2M_{\Lambda_b}^2}{q^2}$ appearing in eqs. (2.10)–(2.13). Therefore the suppression of the “annihilation topologies” is only due the small Wilson coefficients of the operators \mathcal{O}_{3-6} . It is also important to stress that, while local form factors are real-valued, the non-local form factors are generally complex-valued. This is evident in our LCSRs, as there is a pole in the integration path of $d\bar{\omega}_1$. From a phenomenological point of view, this imaginary part is due to $u\bar{u}$ and $d\bar{d}$ hadronic states going on shell. In other words, $\mathcal{H}_{\perp(5)}^{(i)}$ and $\mathcal{H}_{+(5)}^{(i)}$ have a branch cut on the real positive axis starting at $q^2 = 4m_\pi^2$.

It is also interesting to compare our results for $\Lambda_b \rightarrow \Lambda \ell^+ \ell^-$ decays calculated using LCSRs with the corresponding results for $B \rightarrow K^{(*)} \ell^+ \ell^-$ calculated using QCD factorisation, i.e. the annihilation topologies [33, 43]. Confronting our eqs. (3.44)–(3.45) with eq. (18) of ref. [33], we find that the two hard scattering kernels have a very similar structure, with a pole appearing in the denominator for any $q^2 > 0$. Another analogy concerns the fact that in both the mesonic and baryonic cases the leading contribution comes from the diagram where the photon is emitted from the spectator quark in the b hadron. However, as mentioned

Parameter	Value	ref.
f_Λ	$(5.96^{+0.20}_{-0.19}) \cdot 10^{-3} \text{ GeV}^2$	[44]
$f_{\Lambda_b}^{(2)}$	$(3.0 \pm 0.5) \cdot 10^{-2} \text{ GeV}^3$	[40, 45]
s_0	2.55 GeV^2	[21]
$\omega_M(n_+ \cdot p')$	$2.5 \pm 0.5 \text{ GeV}^2$	[21]
$1/\omega_0$	$3.4 \pm 1.6 \text{ MeV}^{-1}$	[21, 22]

Table 1. Input parameters used to evaluate the LCSRs. The lattice QCD calculation of f_Λ in ref. [44] is compatible with an older sum-rule estimate in ref. [46]. Notice that the normalisation convention in ref. [44] differs from that used by us and in ref. [46] by a SU(3) Clebsch-Gordan factor $\sqrt{\frac{3}{2}}$.

above, in the mesonic case the contributing operators are \mathcal{O}_3 and \mathcal{O}_4 , while in the baryonic case they are \mathcal{O}_5 and \mathcal{O}_6 . Also, in the baryonic case only the transverse γ^* polarisation contributes at leading power, while in the mesonic case the dominant annihilation effect appears for longitudinal γ^* polarisation.

4 Numerical results

We provide numerical results for the non-local form factors $\mathcal{H}_{\perp(5)}^{(i)}$ and $\mathcal{H}_{+(5)}^{(i)}$ using the LCSRs in eqs. (3.44) and (3.45) and also taking into account the identities (3.43) (see also appendix B for the integrated LCSRs). These LCSRs are evaluated with the inputs listed in table 1 and the LCDAs models obtained in appendix A. As there is no independent estimate of the LCDA parameter ω_0 , we vary its inverse in the interval $[1.8, 5.0] \text{ MeV}^{-1}$. This very conservative interval contains with margin the estimates of refs. [21, 22]. The interval for the Borel parameter ω_M is chosen in such a way that this parameter is both sufficiently large to suppress higher power corrections in the OPE and sufficiently small to ensure that the contribution of the continuum and excited states is subleading compared to that of the Λ baryon. We use the same central value of ref. [21] and vary it within $\pm 0.5 \text{ GeV}^2$. We have checked that our LCSRs are stable in this interval for the Borel parameter. As in ref. [21], we choose s_0 to be equal to the mass of the next resonance with the same quantum numbers of the Λ baryon. All parameters in table 1 are assumed to be Gaussian distributed, except for the Borel parameter for which we take a flat distribution.

The LCSRs in eqs. (3.44) and (3.45) can be used for values of q^2 such that the energy of the Λ baryon is of the order of $m_{\Lambda_b}/2$ in the Λ_b baryon rest frame. To avoid large violations of the quark-hadron duality, we also take q^2 larger than the narrow vector resonances such as the ρ and ω mesons. We can therefore evaluate our LCSRs in the range $2 \text{ GeV}^2 \lesssim q^2 \lesssim 6 \text{ GeV}^2$. We choose the following q^2 points: $q^2 = \{2, 4, 6\} \text{ GeV}^2$. We obtain

$$\begin{aligned}
 10^5 \cdot \mathcal{H}_{\perp}^{(5)}(2 \text{ GeV}^2) &= -(1.2 \pm 5.6) - i(15.6 \pm 8.2), \\
 10^5 \cdot \mathcal{H}_{\perp}^{(5)}(4 \text{ GeV}^2) &= (6.8 \pm 5.3) - i(8.2 \pm 2.6), \\
 10^5 \cdot \mathcal{H}_{\perp}^{(5)}(6 \text{ GeV}^2) &= (6.5 \pm 3.2) - i(3.9 \pm 1.6),
 \end{aligned}
 \tag{4.1}$$

and

$$\begin{aligned}
10^7 \cdot \mathcal{H}_+^{(5)}(2 \text{ GeV}^2) &= -(1.31 \pm 0.74) + i(1.47 \pm 0.38), \\
10^7 \cdot \mathcal{H}_+^{(5)}(4 \text{ GeV}^2) &= -(2.48 \pm 0.88) + i(1.16 \pm 0.45), \\
10^7 \cdot \mathcal{H}_+^{(5)}(6 \text{ GeV}^2) &= -(3.38 \pm 0.90) + i(0.85 \pm 0.58),
\end{aligned}
\tag{4.2}$$

We remind the reader that the results for the other non-local form factors can be obtained using the identities (3.43). We can cast the results above also in the form of a q^2 -dependent shift to C_9 using eqs. (2.10)–(2.13):

$$\begin{aligned}
10^2 \cdot \Delta C_{9,\perp}(2 \text{ GeV}^2) &= (0.6 \pm 2.5) + i(6.9 \pm 1.3), \\
10^2 \cdot \Delta C_{9,\perp}(4 \text{ GeV}^2) &= -(0.97 \pm 0.98) + i(1.89 \pm 0.62), \\
10^2 \cdot \Delta C_{9,\perp}(6 \text{ GeV}^2) &= -(0.64 \pm 0.39) + i(0.63 \pm 0.42),
\end{aligned}
\tag{4.3}$$

and

$$\begin{aligned}
10^5 \cdot \Delta C_{9,+}(2 \text{ GeV}^2) &= (5.2 \pm 3.1) - i(8.7 \pm 3.8), \\
10^5 \cdot \Delta C_{9,+}(4 \text{ GeV}^2) &= (5.1 \pm 2.2) - i(4.1 \pm 4.0), \\
10^5 \cdot \Delta C_{9,+}(6 \text{ GeV}^2) &= (4.3 \pm 2.1) - i(2.3 \pm 3.7).
\end{aligned}
\tag{4.4}$$

For the local form factors we have used the analytical results of ref. [21], i.e. eqs. (3.46) and (3.47), evaluated with the inputs of table 1. The values of the Wilson coefficients — evaluated at the scale $\mu = m_b$ — are taken from ref. [47].

A few comments on our numerical results are in order:

- As expected from the OPE results obtained in section 3.5, $\mathcal{H}_+^{(5)}$ is power suppressed w.r.t. $\mathcal{H}_\perp^{(5)}$ and this is reflected in the numerical results of eq. (4.1). This makes the contribution of $\mathcal{H}_+^{(5)}$ essentially negligible.
- The uncertainty of our numerical results is dominated by the LCDA model parameter ω_0 . It is therefore crucial to have a better knowledge of the LCDAs and their parameters in order to improve the accuracy of the current calculation.
- We find that $|\Delta C_{9,\perp}|/C_9$ is $\mathcal{O}(1\%)$. This means that if, as expected, the theoretical precision of the local $\Lambda_b \rightarrow \Lambda$ form factors is improved by future lattice QCD calculations [18], the annihilation topologies should be taken into account in the prediction of $\Lambda_b \rightarrow \Lambda \ell^+ \ell^-$ observables.
- Comparing the C_9 shift due to the weak annihilation in $B^+ \rightarrow K^{(*)+} \ell^+ \ell^-$ decays [33, 43, 48], with our $\Delta C_{9,\perp}$, we find that these two different contributions have a very similar q^2 dependence. In particular, both their real parts have a zero at $q^2 \simeq 2 \text{ GeV}^2$, while the imaginary parts are positive definite. Regarding their magnitude, we find $\Delta C_{9,\perp}$ to be about 5 times larger than for $B^+ \rightarrow K^+ \ell^+ \ell^-$ and $B^+ \rightarrow K_{\parallel}^{*+} \ell^+ \ell^-$ decays.

5 Conclusions

In this work, we have studied the non-local contributions of the strong penguin operators in $\Lambda_b \rightarrow \Lambda \ell^+ \ell^+$ decays, where a virtual photon is radiated from one of the light quarks. We refer to this situation as “annihilation topologies” because of the analogy with annihilation in $B \rightarrow K^{(*)} \ell^+ \ell^+$ decays. Their contribution to the corresponding non-local form factors is calculated using light-cone sum rules (LCSRs) with Λ_b light-cone distribution amplitudes (LCDAs). More precisely, we find that — at leading power — the hard-scattering kernel entering the factorisation formula for the underlying correlator depends on opposite light-cone projections of the two light-quark momenta in the Λ_b baryon. This implies that in this case the required hadronic information about the Λ_b bound state is contained in a new type of soft functions that generalise the standard LCDAs which are known in the literature and used, for instance, in local form-factor calculations. In order to evaluate the LCSRs, we have constructed a model for these new soft functions that links them to the standard Λ_b LCDAs. On this basis, we have presented the result from the leading-order LCSRs for the annihilation contribution to the non-local form factors in analytical form. Here we have focused on the leading annihilation topology, where the virtual photon is radiated from one of the light (soft) quarks in the Λ_b baryon. Numerical predictions are presented in the form of a q^2 -dependent shift ΔC_9 of the Wilson coefficient C_9 , where q^2 is the invariant mass of the lepton pair. In the considered range $q^2 \in [2, 6]$, we observe that $|\Delta C_{9,\perp}|/C_9 \sim \mathcal{O}(1\%)$ and $\text{Im}\Delta C_9 \neq 0$, and hence this effect should not be neglected in precision analyses of $\Lambda_b \rightarrow \Lambda \ell^+ \ell^+$ observables.

Our findings show a number of analogies with the annihilation topologies in $B \rightarrow K^{(*)} \ell^+ \ell^+$ decays. For instance, in both cases ΔC_9 features a very similar q^2 dependence and is of similar numerical size, which can be traced back to the functional form of the intermediate hard-collinear light-quark propagator folded with the modelled shape of the (generalised) LCDAs. A major difference is that in the mesonic case the operators of the weak effective Hamiltonian that contribute at leading order are \mathcal{O}_3 and \mathcal{O}_4 (with left-handed $q\bar{q}$ currents), while in the baryonic case they are \mathcal{O}_5 and \mathcal{O}_6 (with right-handed $q\bar{q}$ currents). This can be traced back to the Dirac structure of the penguin operators that results from replacing the light quark fields by their leading spinor components in soft-collinear effective theory.

We re-emphasise that in our analysis we only considered one particular non-factorising decay topology, and it is left for future work to perform similar investigations for the sub-leading annihilation topologies, but also to study related topologies where a quark loop originating from the 4-quark operators or the chromomagnetic penguin operator connects to one of the light quarks from the Λ_b bound state by hard-collinear gluon exchange (similar topologies had been studied for mesonic transition in the past). While in both cases, we expect sub-leading numerical effects, verification by explicit calculation would be desirable.

To conclude, the inclusion of genuinely *non-factorising* contributions from hadronic operators in $\Lambda_b \rightarrow \Lambda \ell^+ \ell^-$ decays at large recoil are important, not only to improve the accuracy of SM predictions for physical observables and to sharpen the current constraints on physics beyond the SM, but also as a laboratory to test our understanding and further deepen our knowledge of non-perturbative QCD effects in exclusive baryonic reactions.

Acknowledgments

We thank Marzia Bordone for her contributions in the early stage of this project. This research is supported by the Deutsche Forschungsgemeinschaft (DFG, German Research Foundation) under grant 396021762 – TRR 257. The work of N.G. has been partially supported by STFC consolidated grants ST/T000694/1 and ST/X000664/1.

A Models for Λ_b LCDAs in momentum space

A straightforward procedure for constructing explicit models for the LCDAs appearing in the momentum-space projector (3.24) has been outlined in ref. [41]. For this purpose, the following ansatz is used

$$M^{(2)}(v, k_1, k_2) = \tilde{\psi}_v(x_1, x_2, K^2) \not{k}_2 \not{v} \not{k}_1, \quad (\text{A.1})$$

where

$$x_i = 2v \cdot k_i, \quad K^2 = (k_1 + k_2)^2. \quad (\text{A.2})$$

In this way the Dirac matrix $M^{(2)}$ automatically fulfils the equations of motion for on-shell light quarks in the Λ_b Fock state.³ We further follow ref. [41] and *assume* that the shape of the wave function ψ_v is predominantly determined by its dependence on the invariant mass of the three-quark bound state, $(m_b v + k_1 + k_2)^2 \simeq m_b^2 + m_b(x_1 + x_2)$, such that the K^2 -dependence can be ignored,

$$\psi_v(x_1, x_2, K^2) \rightarrow \psi_v(x_1, x_2). \quad (\text{A.3})$$

We may then fold the ansatz for the momentum-space projector in (A.1) with a test kernel which includes terms at most linear in the transverse momenta $k_{i\perp}$. Writing

$$\not{k}_1 = \bar{\omega}_1 \frac{\not{p}_-}{2} + (x_1 - \bar{\omega}_1) \frac{\not{p}_+}{2} + \not{k}_1^\perp, \quad \not{k}_2 = \omega_2 \frac{\not{p}_+}{2} + (x_2 - \omega_2) \frac{\not{p}_-}{2} + \not{k}_2^\perp, \quad (\text{A.4})$$

with $k_1^2 = k_2^2 = 0$, this leads to

$$\begin{aligned} & \int \widetilde{dk}_1 \int \widetilde{dk}_2 \text{tr} \left[\left(T_0(\bar{\omega}_1, \omega_2) + k_{i\perp}^\mu T_\mu^i(\bar{\omega}_1, \omega_2) \right) M^{(2)}(v, k_1, k_2) \right] \\ &= \int d\bar{\omega}_1 d\omega_2 \int_{\bar{\omega}_1}^{\infty} dx_1 \int_{\omega_2}^{\infty} dx_2 \left\{ \right. \\ & \quad \text{tr} \left[T_0(\bar{\omega}_1, \omega_2) \left((x_1 - \bar{\omega}_1)\omega_2 \frac{\not{p}_+}{2} + \bar{\omega}_1(x_2 - \omega_2) \frac{\not{p}_-}{2} \right) \right] \\ & \quad - \text{tr} \left[T_\mu^1(\bar{\omega}_1, \omega_2) \left(\bar{\omega}_1\omega_2(x_1 - \bar{\omega}_1) \frac{\not{p}_+\not{p}_-}{4} + \bar{\omega}_1(x_1 - \bar{\omega}_1)(x_2 - \omega_2) \frac{\not{p}_-\not{p}_+}{4} \right) \frac{\gamma_\perp^\mu}{2} \right] \\ & \quad - \text{tr} \left[T_\mu^2(\bar{\omega}_1, \omega_2) \frac{\gamma_\perp^\mu}{2} \left(\omega_2(x_1 - \bar{\omega}_1)(x_2 - \omega_2) \frac{\not{p}_-\not{p}_+}{4} + \bar{\omega}_1\omega_2(x_2 - \omega_2) \frac{\not{p}_+\not{p}_-}{4} \right) \right] \\ & \left. \right\} \psi_v(x_1, x_2), \quad (\text{A.5}) \end{aligned}$$

³The resulting relations between the individual LCDAs/soft functions are sometimes referred to as “Wandzura-Wilczek approximation”. These are valid up to corrections involving the four-particle LCDAs.

where $\widetilde{dk}_i = d^3k_i/(\pi x_i)$ are Lorentz-invariant phase-space integrals for the (massless) light quarks in the Λ_b baryon. Comparing with the momentum-space projector (3.24), one easily obtains

$$\chi_2(\bar{\omega}_1, \omega_2) = \int_{\bar{\omega}_1}^{\infty} dx_1 \int_{\omega_2}^{\infty} dx_2 \left(x_1 \omega_2 + x_2 \bar{\omega}_1 - \bar{\omega}_1 \omega_2 - \frac{x_1 x_2}{2} \right) \psi_v(x_1, x_2), \quad (\text{A.6})$$

and

$$\chi_{42}^{(i)}(\bar{\omega}_1, \omega_2) = \frac{1}{2} \int_{\bar{\omega}_1}^{\infty} dx_1 \int_{\omega_2}^{\infty} dx_2 x_2 (x_1 - 2\bar{\omega}_1) \psi_v(x_1, x_2), \quad (\text{A.7})$$

$$\chi_{42}^{(ii)}(\bar{\omega}_1, \omega_2) = \frac{1}{2} \int_{\bar{\omega}_1}^{\infty} dx_1 \int_{\omega_2}^{\infty} dx_2 x_1 (x_2 - 2\omega_2) \psi_v(x_1, x_2), \quad (\text{A.8})$$

$$\chi_X(\bar{\omega}_1, \omega_2) = \frac{1}{2} \int_{\bar{\omega}_1}^{\infty} dx_1 \int_{\omega_2}^{\infty} dx_2 (x_1 - 2\bar{\omega}_1) (x_2 - 2\omega_2) \psi_v(x_1, x_2). \quad (\text{A.9})$$

A simplified model for the baryon wave functions can then be obtained by assuming an exponential dependence of the wave function ψ_v on $(x_1 + x_2)$ as in refs. [21, 41]:

$$\psi_v(x_1, x_2) := \frac{1}{\omega_0} \exp\left(-\frac{x_1 + x_2}{\omega_0^6}\right). \quad (\text{A.10})$$

For this case, we obtain the following expressions for the linear combinations entering the momentum-space projector,

$$\chi_2(\bar{\omega}_1, \omega_2) + \chi_{42}^{(i)}(\bar{\omega}_1, \omega_2) = \frac{\omega_2}{\omega_0^3} e^{-(\bar{\omega}_1 + \omega_2)/\omega_0}, \quad (\text{A.11})$$

$$\chi_2(\bar{\omega}_1, \omega_2) + \chi_{42}^{(ii)}(\bar{\omega}_1, \omega_2) = \frac{\bar{\omega}_1}{\omega_0^3} e^{-(\bar{\omega}_1 + \omega_2)/\omega_0}, \quad (\text{A.12})$$

$$\bar{\chi}_{42}^{(i)}(\bar{\omega}_1, \omega_2) - \bar{\chi}_X(\bar{\omega}_1, \omega_2) = \frac{\bar{\omega}_1 \omega_2}{\omega_0^3} e^{-(\bar{\omega}_1 + \omega_2)/\omega_0}, \quad (\text{A.13})$$

$$\bar{\chi}_{42}^{(ii)}(\bar{\omega}_1, \omega_2) + \bar{\chi}_X(\bar{\omega}_1, \omega_2) = \frac{\bar{\omega}_1}{\omega_0^2} e^{-(\bar{\omega}_1 + \omega_2)/\omega_0}, \quad (\text{A.14})$$

$$\hat{\chi}_{42}^{(ii)}(\bar{\omega}_1, \omega_2) + \hat{\chi}_X(\bar{\omega}_1, \omega_2) = \frac{\omega_2}{\omega_0^2} e^{-(\bar{\omega}_1 + \omega_2)/\omega_0}, \quad (\text{A.15})$$

$$\hat{\chi}_{42}^{(ii)}(\bar{\omega}_1, \omega_2) - \hat{\chi}_X(\bar{\omega}_1, \omega_2) = \frac{\bar{\omega}_1 \omega_2}{\omega_0^3} e^{-(\bar{\omega}_1 + \omega_2)/\omega_0}. \quad (\text{A.16})$$

B Further details on the LCSRs

In the following, we provide a few intermediate steps in the derivation of the LCSRs in section 3.6, i.e. the matching of the OPE calculation Π_{μ}^{OPE} of eqs. (3.33) and (3.39) onto the respective hadronic representations of eqs. (3.7) and (3.8). This matching yields the LCSRs for the non-local form factors $\mathcal{H}_{\perp(5)}^{(i)}$ and $\mathcal{H}_{+(5)}^{(i)}$. After applying quark-hadron duality and

performing the Borel transform, the resulting LCSRs read

$$\begin{aligned}
 & M_{\Lambda_b}^2 f_{\Lambda}(n_+ \cdot p' - m_{\Lambda}) \frac{\not{h}_-}{2} \left[\mathcal{H}_{\perp}^{(i)}(q^2) \gamma_{\mu}^{\perp} - \mathcal{H}_{\perp 5}^{(i)}(q^2) \gamma_{\mu}^{\perp} \gamma_5 \right] e^{-\frac{m_{\Lambda}^2}{(n_+ \cdot p') \omega_M}} u_{\Lambda_b}(p) = \\
 & \mp \frac{(Q_u + Q_d) f_{\Lambda_b}^{(2)}}{192\pi^2} \int_0^{\sigma_0} d\sigma \int_0^{\sigma} d\omega_2 \int_0^{\infty} d\bar{\omega}_1 \frac{(n_+ \cdot p')^2}{n_+ \cdot q - \bar{\omega}_1 + i\epsilon} \left(\chi_2(\bar{\omega}_1, \omega_2) + \chi_{42}^{(ii)}(\bar{\omega}_1, \omega_2) \right) \\
 & \times \left(-\frac{g_{\mu\nu}^{\perp}}{2} \mp \frac{i\epsilon_{\mu\nu\rho\sigma} n_{-}^{\rho} n_{+}^{\sigma}}{4} \right) e^{-\frac{\sigma}{\omega_M}} \left[\not{h}_- \gamma_{\perp}^{\nu} P_L \right] u_{\Lambda_b}(v), \tag{B.1}
 \end{aligned}$$

and

$$\begin{aligned}
 & -\frac{M_{\Lambda_b}^2}{2q^2} f_{\Lambda}(n_+ \cdot p' + m_{\Lambda}) \\
 & \times \frac{\not{h}_-}{2} \left[s_-(M_{\Lambda_b} + m_{\Lambda}) \mathcal{H}_{+}^{(i)}(q^2) - s_+(M_{\Lambda_b} - m_{\Lambda}) \mathcal{H}_{+5}^{(i)}(q^2) \gamma_5 \right] e^{-\frac{m_{\Lambda}^2}{(n_+ \cdot p') \omega_M}} u_{\Lambda_b}(p) \\
 & = \pm \frac{1}{4} \frac{(Q_u + Q_d) f_{\Lambda_b}^{(2)}}{192\pi} M_{\Lambda_b} \int_0^{\sigma_0} d\sigma \int_0^{\sigma} d\omega_2 \int_0^{\infty} d\bar{\omega}_1 \frac{n_+ \cdot p'}{n_+ \cdot q - \bar{\omega}_1 + i\epsilon} \left(\hat{\chi}_{42}^{(ii)}(\bar{\omega}_1, \omega_2) + \hat{\chi}_X(\bar{\omega}_1, \omega_2) \right) \\
 & \times \left[\gamma_{\beta} \not{h}_- \right] \left(\frac{g_{\perp}^{\beta\nu}}{2} \pm \frac{i\epsilon^{\beta\nu\{n_+\}\{n_-\}}}{4} \right) \left[\not{h}_+ \gamma_{\nu} P_L \right] e^{-\frac{\sigma}{\omega_M}} u_{\Lambda_b}(v). \tag{B.2}
 \end{aligned}$$

Here $\sigma_{(0)} \equiv s_{(0)}/(n_+ \cdot p')$ and we have also added the contribution of the diagram where the photon is emitted from the d quark instead of the u quark, resulting in the total charge factor $(Q_u + Q_d)$. It is a straightforward task to derive the identities (3.43) from these LCSRs using eqs. (3.34), (3.35), (3.40), and (3.41).

Using the model for the LCDAs presented in appendix A, it is possible to perform all integrations over light-cone momenta analytically. Here, one has to take into account that, the integration over $d\bar{\omega}_1$ contains a singularity on the integration path for $\epsilon \rightarrow 0$. These integrals can be performed by Cauchy's theorem, along the same lines as for the annihilation in $B \rightarrow K^{(*)} \ell^+ \ell^-$ [33], leading to

$$\begin{aligned}
 \mathcal{H}_{\perp}^{(5)}(q^2) &= \frac{f_{\Lambda_b}^{(2)} (Q_u + Q_d)}{f_{\Lambda}} \frac{\omega_M (n_+ \cdot p')^2}{192\pi^2 M_{\Lambda_b}^2 (n_+ \cdot p' - m_{\Lambda})} \frac{\omega_0 \left(e^{\frac{\sigma_0}{\omega_0}} - 1 \right) - \omega_M e^{\frac{\sigma_0}{\omega_0}} \left(e^{\frac{\sigma_0}{\omega_M}} - 1 \right)}{\omega_0^2 (\omega_0 + \omega_M)} \\
 & \times \left(\omega_0 e^{\frac{M_{\Lambda_b}}{\omega_0}} + (n_+ \cdot p' - M_{\Lambda_b}) e^{\frac{n_+ \cdot p'}{\omega_0}} \left(\text{Ei} \left(\frac{M_{\Lambda_b} - n_+ \cdot p'}{\omega_0} \right) - i\pi \right) \right) \\
 & \times e^{\frac{m_{\Lambda}^2 - \sigma_0 n_+ \cdot p'}{\omega_M n_+ \cdot p'} - \frac{M_{\Lambda_b} + \sigma_0}{\omega_0}}, \tag{B.3}
 \end{aligned}$$

and

$$\begin{aligned}
 \mathcal{H}_{+}^{(5)}(q^2) &= \frac{f_{\Lambda_b}^{(2)} (Q_u + Q_d)}{f_{\Lambda}} \frac{\omega_M n_+ \cdot p'}{192\pi^2 s_-(m_{\Lambda} + M_{\Lambda_b})} \frac{n_+ \cdot p' - M_{\Lambda_b}}{m_{\Lambda} + n_+ \cdot p'} \frac{\text{Ei} \left(\frac{M_{\Lambda_b} - n_+ \cdot p'}{\omega_0} \right) - i\pi}{(\omega_0 + \omega_M)^2} \\
 & \times \left((\omega_0^2 + 2\omega_0 \omega_M) \left(1 - e^{\frac{\sigma_0}{\omega_0}} \right) - \omega_M^2 e^{\frac{\sigma_0}{\omega_0}} \left(1 - e^{\frac{\sigma_0}{\omega_M}} \right) + \sigma_0 (\omega_0 + \omega_M) \right) \\
 & \times e^{\frac{m_{\Lambda}^2 - \sigma_0 n_+ \cdot p'}{\omega_M n_+ \cdot p'} - \frac{M_{\Lambda_b} - n_+ \cdot p' + \sigma_0}{\omega_0}}, \tag{B.4}
 \end{aligned}$$

where $\text{Ei}(x)$ is the exponential integral function.

Open Access. This article is distributed under the terms of the Creative Commons Attribution License ([CC-BY4.0](https://creativecommons.org/licenses/by/4.0/)), which permits any use, distribution and reproduction in any medium, provided the original author(s) and source are credited.

References

- [1] LHCb collaboration, *Implications of LHCb measurements and future prospects*, *Eur. Phys. J. C* **73** (2013) 2373 [[arXiv:1208.3355](https://arxiv.org/abs/1208.3355)] [[INSPIRE](#)].
- [2] BELLE-II collaboration, *The Belle II Physics Book*, *PTEP* **2019** (2019) 123C01 [*Erratum ibid.* **2020** (2020) 029201] [[arXiv:1808.10567](https://arxiv.org/abs/1808.10567)] [[INSPIRE](#)].
- [3] M. Beneke, G. Buchalla, M. Neubert and C.T. Sachrajda, *QCD factorization for $B \rightarrow \pi\pi$ decays: Strong phases and CP violation in the heavy quark limit*, *Phys. Rev. Lett.* **83** (1999) 1914 [[hep-ph/9905312](https://arxiv.org/abs/hep-ph/9905312)] [[INSPIRE](#)].
- [4] M. Beneke, G. Buchalla, M. Neubert and C.T. Sachrajda, *QCD factorization for exclusive, nonleptonic B meson decays: General arguments and the case of heavy light final states*, *Nucl. Phys. B* **591** (2000) 313 [[hep-ph/0006124](https://arxiv.org/abs/hep-ph/0006124)] [[INSPIRE](#)].
- [5] M. Beneke, G. Buchalla, M. Neubert and C.T. Sachrajda, *QCD factorization in $B \rightarrow \pi K, \pi\pi$ decays and extraction of Wolfenstein parameters*, *Nucl. Phys. B* **606** (2001) 245 [[hep-ph/0104110](https://arxiv.org/abs/hep-ph/0104110)] [[INSPIRE](#)].
- [6] A. Khodjamirian, B. Melić and Y.-M. Wang, *A guide to the QCD light-cone sum rule for b-quark decays*, [arXiv:2311.08700](https://arxiv.org/abs/2311.08700) [[DOI:10.1140/epjs/s11734-023-01046-6](https://doi.org/10.1140/epjs/s11734-023-01046-6)] [[INSPIRE](#)].
- [7] C.W. Bauer, S. Fleming, D. Pirjol and I.W. Stewart, *An effective field theory for collinear and soft gluons: Heavy to light decays*, *Phys. Rev. D* **63** (2001) 114020 [[hep-ph/0011336](https://arxiv.org/abs/hep-ph/0011336)] [[INSPIRE](#)].
- [8] C.W. Bauer, D. Pirjol and I.W. Stewart, *Soft collinear factorization in effective field theory*, *Phys. Rev. D* **65** (2002) 054022 [[hep-ph/0109045](https://arxiv.org/abs/hep-ph/0109045)] [[INSPIRE](#)].
- [9] M. Beneke, A.P. Chapovsky, M. Diehl and T. Feldmann, *Soft collinear effective theory and heavy to light currents beyond leading power*, *Nucl. Phys. B* **643** (2002) 431 [[hep-ph/0206152](https://arxiv.org/abs/hep-ph/0206152)] [[INSPIRE](#)].
- [10] J. Albrecht, D. van Dyk and C. Langenbruch, *Flavour anomalies in heavy quark decays*, *Prog. Part. Nucl. Phys.* **120** (2021) 103885 [[arXiv:2107.04822](https://arxiv.org/abs/2107.04822)] [[INSPIRE](#)].
- [11] B. Capdevila, A. Crivellin and J. Matias, *Review of Semileptonic B Anomalies*, *Eur. Phys. J. ST* **1** (2023) 20 [[arXiv:2309.01311](https://arxiv.org/abs/2309.01311)] [[INSPIRE](#)].
- [12] LHCb collaboration, *Angular moments of the decay $\Lambda_b^0 \rightarrow \Lambda\mu^+\mu^-$ at low hadronic recoil*, *JHEP* **09** (2018) 146 [[arXiv:1808.00264](https://arxiv.org/abs/1808.00264)] [[INSPIRE](#)].
- [13] T. Gutsche et al., *Rare baryon decays $\Lambda_b \rightarrow \Lambda l^+ l^-$ ($l = e, \mu, \tau$) and $\Lambda_b \rightarrow \Lambda\gamma$: differential and total rates, lepton- and hadron-side forward-backward asymmetries*, *Phys. Rev. D* **87** (2013) 074031 [[arXiv:1301.3737](https://arxiv.org/abs/1301.3737)] [[INSPIRE](#)].
- [14] P. Böer, T. Feldmann and D. van Dyk, *Angular Analysis of the Decay $\Lambda_b \rightarrow \Lambda(\rightarrow N\pi)\ell^+\ell^-$* , *JHEP* **01** (2015) 155 [[arXiv:1410.2115](https://arxiv.org/abs/1410.2115)] [[INSPIRE](#)].
- [15] T. Blake, S. Meinel and D. van Dyk, *Bayesian Analysis of $b \rightarrow s\mu^+\mu^-$ Wilson Coefficients using the Full Angular Distribution of $\Lambda_b \rightarrow \Lambda(\rightarrow p\pi^-)\mu^+\mu^-$ Decays*, *Phys. Rev. D* **101** (2020) 035023 [[arXiv:1912.05811](https://arxiv.org/abs/1912.05811)] [[INSPIRE](#)].

- [16] M. Algueró et al., $b \rightarrow s\ell^+\ell^-$ global fits after R_{K_S} and $R_{K^{*+}}$, *Eur. Phys. J. C* **82** (2022) 326 [[arXiv:2104.08921](#)] [[INSPIRE](#)].
- [17] W. Detmold and S. Meinel, $\Lambda_b \rightarrow \Lambda\ell^+\ell^-$ form factors, differential branching fraction, and angular observables from lattice QCD with relativistic b quarks, *Phys. Rev. D* **93** (2016) 074501 [[arXiv:1602.01399](#)] [[INSPIRE](#)].
- [18] S. Meinel, Status of next-generation $\Lambda_b \rightarrow p, \Lambda, \Lambda_c$ form-factor calculations, *PoS LATTICE2023* (2024) 275 [[arXiv:2309.01821](#)] [[INSPIRE](#)].
- [19] Y.-M. Wang, Y.-L. Shen and C.-D. Lu, $\Lambda_{(b)} \rightarrow p, \Lambda$ transition form factors from QCD light-cone sum rules, *Phys. Rev. D* **80** (2009) 074012 [[arXiv:0907.4008](#)] [[INSPIRE](#)].
- [20] T.M. Aliev, K. Azizi and M. Savci, Analysis of the $\Lambda_b \rightarrow \Lambda\ell^+\ell^-$ decay in QCD, *Phys. Rev. D* **81** (2010) 056006 [[arXiv:1001.0227](#)] [[INSPIRE](#)].
- [21] T. Feldmann and M.W.Y. Yip, Form factors for $\Lambda_b \rightarrow \Lambda$ transitions in the soft-collinear effective theory, *Phys. Rev. D* **85** (2012) 014035 [Erratum *ibid.* **86** (2012) 079901] [[arXiv:1111.1844](#)] [[INSPIRE](#)].
- [22] Y.-M. Wang and Y.-L. Shen, Perturbative Corrections to $\Lambda_b \rightarrow \Lambda$ Form Factors from QCD Light-Cone Sum Rules, *JHEP* **02** (2016) 179 [[arXiv:1511.09036](#)] [[INSPIRE](#)].
- [23] T. Blake, S. Meinel, M. Rahimi and D. van Dyk, Dispersive bounds for local form factors in $\Lambda_b \rightarrow \Lambda$ transitions, *Phys. Rev. D* **108** (2023) 094509 [[arXiv:2205.06041](#)] [[INSPIRE](#)].
- [24] T. Mannel and S. Recksiegel, Flavor changing neutral current decays of heavy baryons: The Case $\Lambda_{(b)} \rightarrow \Lambda\gamma$, *J. Phys. G* **24** (1998) 979 [[hep-ph/9701399](#)] [[INSPIRE](#)].
- [25] T. Mannel and Y.-M. Wang, Heavy-to-light baryonic form factors at large recoil, *JHEP* **12** (2011) 067 [[arXiv:1111.1849](#)] [[INSPIRE](#)].
- [26] W. Wang, Factorization of Heavy-to-Light Baryonic Transitions in SCET, *Phys. Lett. B* **708** (2012) 119 [[arXiv:1112.0237](#)] [[INSPIRE](#)].
- [27] T. Feldmann, B. Müller and D. Seidel, $D \rightarrow \rho\ell^+\ell^-$ decays in the QCD factorization approach, *JHEP* **08** (2017) 105 [[arXiv:1705.05891](#)] [[INSPIRE](#)].
- [28] C. Bobeth, M. Chrzaszcz, D. van Dyk and J. Virto, Long-distance effects in $B \rightarrow K^*\ell\ell$ from analyticity, *Eur. Phys. J. C* **78** (2018) 451 [[arXiv:1707.07305](#)] [[INSPIRE](#)].
- [29] N. Gubernari, D. van Dyk and J. Virto, Non-local matrix elements in $B_{(s)} \rightarrow \{K^{(*)}, \phi\}\ell^+\ell^-$, *JHEP* **02** (2021) 088 [[arXiv:2011.09813](#)] [[INSPIRE](#)].
- [30] N. Gubernari, M. Reboud, D. van Dyk and J. Virto, Improved theory predictions and global analysis of exclusive $b \rightarrow s\mu^+\mu^-$ processes, *JHEP* **09** (2022) 133 [[arXiv:2206.03797](#)] [[INSPIRE](#)].
- [31] F. De Fazio, T. Feldmann and T. Hurth, Light-cone sum rules in soft-collinear effective theory, *Nucl. Phys. B* **733** (2006) 1 [Erratum *ibid.* **800** (2008) 405] [[hep-ph/0504088](#)] [[INSPIRE](#)].
- [32] A. Khodjamirian, T. Mannel and N. Offen, Form-factors from light-cone sum rules with B -meson distribution amplitudes, *Phys. Rev. D* **75** (2007) 054013 [[hep-ph/0611193](#)] [[INSPIRE](#)].
- [33] M. Beneke, T. Feldmann and D. Seidel, Systematic approach to exclusive $B \rightarrow V\ell^+\ell^-$, $V\gamma$ decays, *Nucl. Phys. B* **612** (2001) 25 [[hep-ph/0106067](#)] [[INSPIRE](#)].
- [34] J. Chay, C. Kim, A.K. Leibovich and J. Zupan, Probing electroweak physics using $B \rightarrow XM$ decays in the endpoint region, *Phys. Rev. D* **76** (2007) 094031 [[arXiv:0708.2466](#)] [[INSPIRE](#)].
- [35] M. Benzke, S.J. Lee, M. Neubert and G. Paz, Factorization at Subleading Power and Irreducible Uncertainties in $\bar{B} \rightarrow X_s\gamma$ Decay, *JHEP* **08** (2010) 099 [[arXiv:1003.5012](#)] [[INSPIRE](#)].

- [36] A. Kozachuk and D. Melikhov, *Revisiting nonfactorizable charm-loop effects in exclusive FCNC B-decays*, *Phys. Lett. B* **786** (2018) 378 [[arXiv:1805.05720](#)] [[INSPIRE](#)].
- [37] M. Beneke, P. Böer, J.-N. Toelstede and K.K. Vos, *Light-cone distribution amplitudes of heavy mesons with QED effects*, *JHEP* **08** (2022) 020 [[arXiv:2204.09091](#)] [[INSPIRE](#)].
- [38] Q. Qin, Y.-L. Shen, C. Wang and Y.-M. Wang, *Deciphering the long-distance penguin contribution to $\bar{B}_{a,s} \rightarrow \gamma\gamma$ decays*, *Phys. Rev. Lett.* **131** (2023) 091902 [[arXiv:2207.02691](#)] [[INSPIRE](#)].
- [39] M.L. Piscopo and A.V. Rusov, *Non-factorisable effects in the decays $\bar{B}_s^0 \rightarrow D_s^+ \pi^-$ and $\bar{B}^0 \rightarrow D^+ K^-$ from LCSR*, *JHEP* **10** (2023) 180 [[arXiv:2307.07594](#)] [[INSPIRE](#)].
- [40] P. Ball, V.M. Braun and E. Gardi, *Distribution Amplitudes of the Λ_b Baryon in QCD*, *Phys. Lett. B* **665** (2008) 197 [[arXiv:0804.2424](#)] [[INSPIRE](#)].
- [41] G. Bell, T. Feldmann, Y.-M. Wang and M.W.Y. Yip, *Light-Cone Distribution Amplitudes for Heavy-Quark Hadrons*, *JHEP* **11** (2013) 191 [[arXiv:1308.6114](#)] [[INSPIRE](#)].
- [42] P. Colangelo and A. Khodjamirian, *QCD sum rules, a modern perspective*, [hep-ph/0010175](#) [[DOI:10.1142/9789812810458_0033](#)] [[INSPIRE](#)].
- [43] C. Bobeth, G. Hiller and G. Piranishvili, *Angular distributions of $\bar{B} \rightarrow \bar{K} \ell^+ \ell^-$ decays*, *JHEP* **12** (2007) 040 [[arXiv:0709.4174](#)] [[INSPIRE](#)].
- [44] RQCD collaboration, *Light-cone distribution amplitudes of octet baryons from lattice QCD*, *Eur. Phys. J. A* **55** (2019) 116 [[arXiv:1903.12590](#)] [[INSPIRE](#)].
- [45] S. Groote, J.G. Körner and O.I. Yakovlev, *An analysis of diagonal and nondiagonal QCD sum rules for heavy baryons at next-to-leading order in alpha-s*, *Phys. Rev. D* **56** (1997) 3943 [[hep-ph/9705447](#)] [[INSPIRE](#)].
- [46] Y.-L. Liu and M.-Q. Huang, *Distribution amplitudes of Sigma and Lambda and their electromagnetic form factors*, *Nucl. Phys. A* **821** (2009) 80 [[arXiv:0811.1812](#)] [[INSPIRE](#)].
- [47] G. Buchalla, A.J. Buras and M.E. Lautenbacher, *Weak decays beyond leading logarithms*, *Rev. Mod. Phys.* **68** (1996) 1125 [[hep-ph/9512380](#)] [[INSPIRE](#)].
- [48] A. Khodjamirian, T. Mannel and Y.M. Wang, *$B \rightarrow K \ell^+ \ell^-$ decay at large hadronic recoil*, *JHEP* **02** (2013) 010 [[arXiv:1211.0234](#)] [[INSPIRE](#)].